Syntheses and Structures of Buta-1,3-Diynyl Complexes from 'On Complex' Cross-Coupling Reactions

Journal:	*Organometallics*
Manuscript ID:	om-2014-01186c.R1
Manuscript Type:	Article
Date Submitted by the Author:	01-Feb-2015
Complete List of Authors:	Oerthel, Marie-Christine; Durham University, Department of Chemistry Yufit, Dmitry; University of Durham, Chemistry Fox, Mark; University of Durham, Department of Chemistry Bryce, Martin; University of Durham, Chemistry Low, Paul; University of Western Australia, School of Chemistry and Biochemistry

Syntheses and Structures of Buta-1,3-Diynyl Complexes from 'On Complex' Cross-Coupling Reactions

Marie-Christine Oerthel,[†] *Dmitry S. Yufit,*[†] *Mark A. Fox,*[†] *Martin R. Bryce,**[†] *Paul J. Low**[‡]

[†] *Department of Chemistry, Durham University, South Rd, Durham, DH1 3LE, UK*

[‡] *School of Chemistry and Biochemistry, University of Western Australia, 35 Stirling Highway, Crawley, Perth 6009, Australia*

Email: m.r.bryce@durham.ac.uk, paul.low@uwa.edu.au

ABSTRACT

The $Pd(PPh_3)_4$ / CuI co-catalyzed reaction of $Ru(C{\equiv}CC{\equiv}CH)(PPh_3)_2Cp$ (**2**) with aryl iodides, Ar-I (**3** Ar = C_6H_4CN-4 (**a**); C_6H_4Me-4 (**b**); C_6H_4OMe-4 (**c**); 2,3-dihydrobenzo[*b*]thiophene (**d**); C_5H_4N (**e**)) proceeds smoothly in diisopropylamine and under an inert atmosphere to give the substituted buta-1,3-diynyl complexes $Ru(C{\equiv}CC{\equiv}CAr)(PPh_3)_2Cp$ (**4a - e**) in moderate to good yield. The procedure allows the rapid preparation of a range of metal complexes of arylbuta-1,3-diynyl ligands without necessitating the prior synthesis of the individual buta-1,3-diynes as ligand precursors. Similar reaction of **2** with half an equivalent of 1,4-diiodobenzene affords the bimetallic derivative $\{Ru(PPh_3)_2Cp\}_2(\mu\text{-}C{\equiv}CC{\equiv}C\text{-}1,4\text{-}C_6H_4\text{-}C{\equiv}CC{\equiv}C)$ (**5**). In the presence of atmospheric oxygen, homocoupling of the diynyl reagent **2** takes place to provide the

octa-1,3,5,7-tetrayndiyl complex $\{Ru(PPh_3)_2Cp\}_2(\mu\text{-}C{\equiv}CC{\equiv}CC{\equiv}CC{\equiv}C)$ (**6**). Crystallographically determined molecular structures are reported for five complexes (**4a**, **4b**, **4d**, **5** and **6**). Quantum chemical calculations indicate that the HOMOs are mainly located on the C_4-C_6H_4-C_4 and C_8 bridges for **5** and **6** respectively, whilst spectroelectrochemical (UV-vis-NIR and IR) studies on **6** establish that oxidation takes place at the C_8 bridge, likely followed by cyclodimerization reactions of the bridging ligand.

INTRODUCTION

Metal oligo/polyynyl $M\{(C{\equiv}C)_nH\}L_x$ species have attracted significant interest over several decades, serving as scaffolds for the assembly of bi-[1-13] and poly-metallic[14-26] complexes, and as models and building blocks for metallomacrocycles,[15, 27-29] and metallo-polymers.[30-35] Detailed studies of the underlying electronic structure of this family of complexes have been undertaken, using a variety of computational and spectroscopic methods, often with a view to modelling the behavior of these prototypical molecular wires.[21,36-39] The terminal C≡CH moiety in polyynyl complexes $M\{(C{\equiv}C)_{n\text{-}1}C{\equiv}CH\}L_x$ offers a convenient entry point for the preparation of a wide range of polyynyl derivatives; however, the functionalization reactions of $\text{-}(C{\equiv}C)_{n\text{-}1}C{\equiv}CH$ ligands are largely based on deprotonation and subsequent trapping with various electrophiles,[9,40-44] including metal complex electrophiles.[45,46]

To the best of our knowledge, the use of the Sonogashira cross-coupling reaction as a tool to prepare substituted derivatives of buta-1,3-diyl complexes was first demonstrated in

reactions of $W(C{\equiv}CC{\equiv}CH)(CO)_3Cp$ with iodoaromatics.[47] However, despite further successful demonstrations of this 'chemistry on the complex' concept to functionalize[48-52] or extend[53-64] metal-alkynyl ligands through homo or cross-coupling protocols, the use of cross-coupling reactions to functionalize metal complexes[65] has been largely overlooked for the preparation of more functional metal alkynyl complexes. More conventional strategies involving the metallation of pre-formed alkynes and (poly)ynes of general form $H(C{\equiv}C)_{n-1}C{\equiv}CR$ or $Me_3Si(C{\equiv}C)_{n-1}C{\equiv}CR$[8,66-69] have been preferred.

We now report the use of Sonogashira-style cross-coupling reactions in the preparation of a range of ruthenium buta-1,3-diynyl complexes from a common $Ru(C{\equiv}CC{\equiv}CH)(PPh_3)_2Cp$ platform. This strategy obviates the need to prepare different diyne ligands for each and every complex, providing rapid access to a range of complexes with various aryl buta-1,3-diynyl ligands.

RESULTS AND DISCUSSION

Fluoride-induced desilylation of the readily-available complex $Ru(C{\equiv}CC{\equiv}CSiMe_3)(PPh_3)_2Cp$ (**1**) affords the terminal buta-1,3-diyl complex $Ru(C{\equiv}CC{\equiv}CH)(PPh_3)_2Cp$ (**2**),[18] which was chosen as a suitable platform on which to test Sonogashira cross-coupling reactions with a wider range of aryliodides **3** than explored previously on the $W(C{\equiv}CC{\equiv}CH)(CO)_3Cp$ platform (Scheme 1).[47]

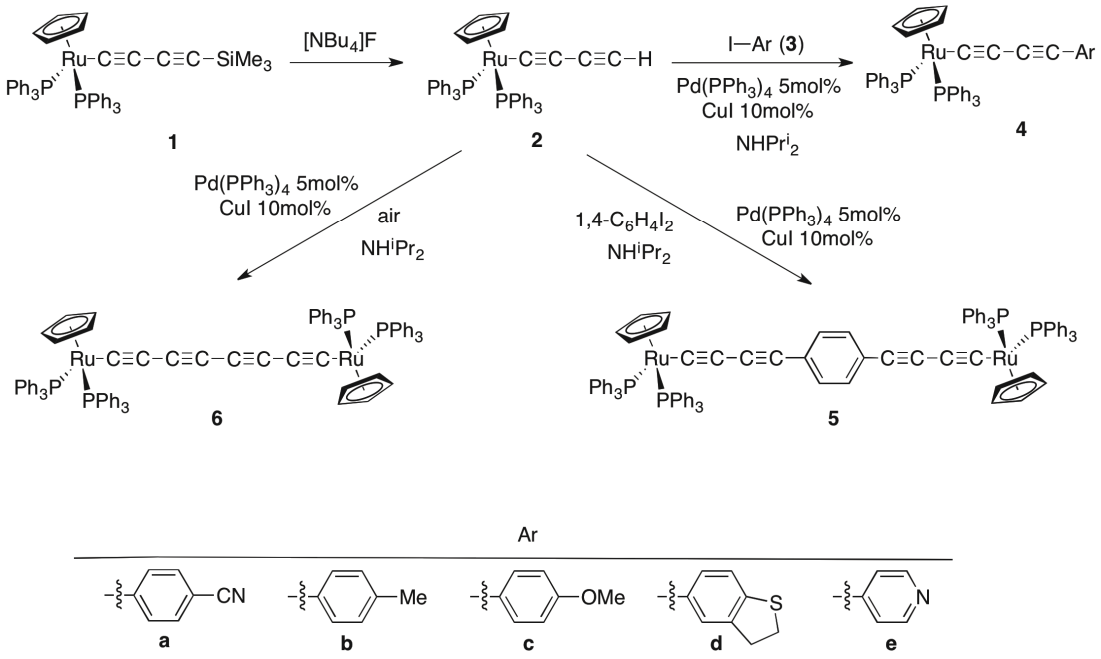

Scheme 1. The Sonogashira cross-coupling reactions of **2** with aryliodides **3a** - **e** yielding **4a** – **e**, and related syntheses of **5** and **6**.

Reaction of **2** with the aryl iodides **3a**-**e** in diisopropylamine co-catalyzed by a simple $Pd(PPh_3)_4$ (5 mol%) / CuI (10 mol%) mixture gave the substituted buta-1,3-diynyl complexes $Ru(C{\equiv}CC{\equiv}CAr)(PPh_3)_2Cp$ **4a** - **e** in moderate (**4a**, 47%; **4c**, 59%; **4d**, 54%; **4e**, 60%) to good (**4b**, 87%) yields. These examples illustrate the versatility of the 'chemistry-on-complex' strategy; through this approach buta-1,3-diynyl complexes with electron-withdrawing (**3a** C_6H_4CN), electro-neutral (**3b** C_6H_4Me), electron-donating (**3c** C_6H_4OMe) or metal surface contacting (**3d** 2,3-dihydrobenzo[*b*]thiophene (DHBT); **3e** C_5H_4N) substituents have been obtained. Similarly, reaction of **2** with one-half equivalent of 1,4-diiodobenzene gave the bimetallic bis(butadiynyl) complex $\{Ru(PPh_3)_2Cp\}_2(\mu$-$C{\equiv}CC{\equiv}C$-1,4-$C_6H_4C{\equiv}CC{\equiv}C)$ (**5**) in 67% yield.

The products were obtained in good purity as precipitates from the reaction mixtures and, where necessary, further purification was achieved by column chromatography and / or crystallization. Identification of the products was readily achieved through a combination of IR, ^{1}H, ^{13}C and ^{31}P NMR spectroscopies, MALDI-TOF and high-resolution ES mass spectrometry. The phosphine ligands were detected in the ^{31}P NMR spectra as singlets in the narrow range 48.2 (**4a**) - 49.1 (**4c**) ppm, whilst the Cp ligands were detected in the ^{1}H spectra between 4.33 - 4.38 ppm. The ^{13}C NMR resonances were assigned with aid of values obtained from calculations modeled on **4a**. In all cases the buta-1,3-diynyl ligand gave rise to a two-band ν(C≡CC≡CAr) pattern with absorptions near 2160 and 2020 cm^{-1} that can be approximated as the local oscillations of the C≡CAr and Ru-C≡C fragments, respectively.[70] In each case the MALDI-TOF spectrum contained the molecular ion, together with a fragment ion derived from loss of PPh_3 in some cases.

Although most commonly used as a cross-coupling methodology, it is well-known that the Sonogashira cycle can be intercepted by oxidants to promote homo-coupling of the terminal alkyne.[71-74] Indeed, Sonogashira-like conditions in the presence of an additional oxidant are emerging as a viable alternative to the Glaser-Hay type methods of 1,3-diyne synthesis.[75] Accordingly, the reaction of **2** with catalytic $Pd(PPh_3)_4$ / CuI in $NHPr^{i}_2$ in an open flask proceeded rapidly to give the homo-coupled octa-1,3,5,7-tetrayndiyl complex $\{Ru(PPh_3)_2Cp\}_2(\mu\text{-}C{\equiv}CC{\equiv}CC{\equiv}CC{\equiv}C)$ (**6**, 55%). Complex **6** (60%)[76] and the closely related buta-1,3-diyndiyl $\{Ru(PPh_3)_2Cp\}_2(\mu\text{-}C{\equiv}CC{\equiv}C)$ and hexa-1,3,5-

triyndiyl{$Ru(PPh_3)_2Cp$}$_2$(μ-C≡CC≡CC≡C)[77] complexes have previously been prepared from desilylation / metallation reactions of the appropriate di-, tri- or tetra-yne Me_3Si-$(C≡C)_n$-$SiMe_3$ with $RuCl(PPh_3)_2Cp$ in presence of KF. Other octa-1,3,5,7-tetrayndiyl complexes have been prepared from oxidative Hay or Glaser style coupling of buta-1,3-diynyl complexes,[2,58,60,78-82] and the approach described here provides a complementary, and highly convenient route to these systems.

Molecular Structures. Single crystals suitable for X-ray diffraction analysis were obtained for the buta-1,3-diynyl complexes **4a**, **4b**, **4d** and bimetallic complexes **5**•CH_2Cl_2 and **6**•$2CH_2Cl_2$; the structure of **6**•$4CHCl_3$ has been reported recently by Bruce and colleagues.[82] Representative plots of **4a**, **5**•CH_2Cl_2 and **6**•$2CH_2Cl_2$ showing the atom labeling scheme are given in Figures 1 - 3, and selected bond lengths and angles for **4a**, **4b**, **4d**, **5**•CH_2Cl_2, **6**•$2CH_2Cl_2$ are summarized in Table 1 together with data from **6**•$4CHCl_3$[82] and DFT optimized structures (vide infra). The diynyl complexes **4a**, **4b** and **4d** featuring the $Ru(PPh_3)_2Cp$ fragment display bond lengths associated with both the diynyl ligand and the metallic half-sandwich moiety that barely differ from the few other examples of Ru(C≡CC≡CR)$(PPh_3)_2Cp$ compounds reported to date: (R = $SiMe_3$,[18] $C(Ph)CBr_2$,[69] Ph,[77] and CN[83]). Thus, the ruthenium centers have the usual pseudo-octahedral geometry, with bond lengths and angles in the ranges: Ru-P 2.284(1) – 2.342(2) Å and P(1)-Ru-P(2) 96.42(8) – 101.39(1)°, P(1,2)-Ru-C(1) 88.37(6) - 92.24(5)°. The Ru-C(1) lengths fall between 1.984(2) Å (**4a**) and 2.002(3) Å (**4b**) which compares with the 1.986(4) - 1.99(1) Å range found in previous examples. For the diynyl chain, the bond lengths display the expected pattern of short-long alternation: C(1)-C(2) 1.21(1) -

1.23(1) Å; C(2)-C(3) 1.35(1) - 1.38(1) Å; C(3)-C(4) 1.168(14) - 1.216(4) Å; and the chain is essentially linear, with angles: Ru-C(1)-C(2) 172.8(2) - 175.6(3)°; C(1)-C(2)-C(3) 170(1) - 178(1)°.

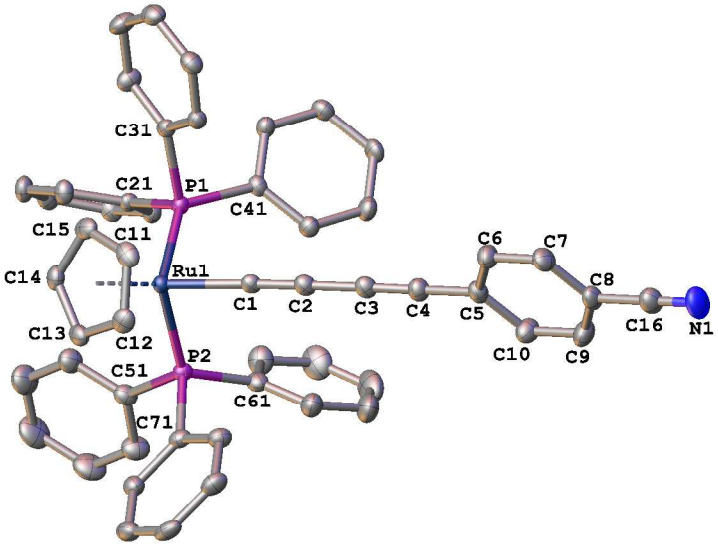

Fig.1 Molecular structure of **4a** showing the atom labeling scheme. In this and all subsequent plots thermal ellipsoids are drawn at 50% probability level, H-atoms and solvent molecules (when present) are omitted for clarity.

Table 1. Selected crystallographically determined bond lengths (Å) and angles (º) for complexes **4a**, **4b**, **4d**, **5**•CH_2Cl_2 and **6**•$2CH_2Cl_2$, with related data from **6**•$4CHCl_3$ and DFT optimized (B3LYP/3-21G*/CPCM-CH_2Cl_2) geometries (**4a´**, **5´** and **6´**)

Bond lengths (Å)	**4a**	**4a´**	**4b**	**4d**	**5**•CH_2Cl_2	**5´**	**6**•$2CH_2Cl_2$	**6**•$4CHCl_3$[82]	**6´**
Ru-P(1)	2.2936(5)	2.3366	2.2884(8)	2.2844 (5)	2.342(2)	2.3324, 2.3344	2.298(2)	2.305(2)	2.3432, 2.3432
Ru-P(2)	2.2915(5)	2.3315	2.3001(7)	2.3088 (5)	2.306(3)	2.3245, 2.3233	2.282(2)	2.291(2)	2.3404, 2.3314
Ru-C(1)	1.984(2)	1.9783	2.002(3)	1.9947 (19)	1.965(10)	1.9855, 1.9860	1.976(5)	1.963(6)	1.9822, 1.9841
C(1)-C(2)	1.221(3)	1.2420	1.214(4)	1.226 (3)	1.233(13)	1.2406, 1.2407	1.229(7)	1.237(7)	1.2440, 1.2445
C(2)-C(3)	1.371(3)	1.3485	1.380(4)	1.373 (3)	1.346(14)	1.3519, 1.3519	1.362(8)	1.370(8)	1.3445, 1.3444
C(3)-C(4)	1.204(3)	1.2255	1.216(4)	1.211 (3)	1.168(14)	1.2250, 1.2250	1.220(7)	1.197(7)	1.2345, 1.2346
C(4)-C(5) / C(4)-C(4´)	1.430(3)	1.4139	1.429(4)	1.431 (3)	1.476(16)	1.4174, 1.4175	1.358(11)	1.385(12)	1.3395
Angles (°)									
P(1)-Ru-P(2)	101.39(2)	102.63	98.89(3)	97.44(2)	96.42(8)	101.07, 101.23	100.27(5)	98.74(4)	101.95, 100.35
P(1)-Ru-C(1)	90.67(5)	90.96	89.89(9)	92.24(5)	93.9(3)	91.07, 91.46	86.49(15)	87.2(1)	88.35, 92.20
P(2)-Ru-C(1)	88.37(6)	88.24	91.77(8)	91.85(5)	90.1(3)	91.13, 90.71	94.12(16)	93.5(1)	92.07, 89.76
Ru-C(1)-C(2)	175.0(2)	175.10	175.6(3)	172.8(2)	172.8(8)	173.91, 173.86	168.5(5)	174.6(4)	173.17, 175.94
C(1)-C(2)-C(3)	178.6(2)	179.21	173.5(3)	174.9(2)	170.3(12)	178.95, 179.03	170.3(6)	173.6(5)	178.35, 178.76
C(2)-C(3)-C(4)	178.3(2)	179.63	177.9(3)	178.2(2)	176.2(12)	179.24, 179.87	175.0(6)	176.7(5)	178.97, 179.08
C(3)-C(4)-C(5)/C(3)-C(4)-C(4´)	173.4(2)	179.63	173.6(3)	179.4(2)	177.2(13)	179.11, 179.35	179.8(8)	178.3(7)	179.05

In the solid state, the bimetallic complexes **5**•CH_2Cl_2 and **6**•$2CH_2Cl_2$ adopt a *trans*-conformation of the Cp rings. The torsion angle C(0)-Ru-C(5)-C(6) is 172.9(9)° (C(0) is the centroid of the Cp ring) suggesting that, at least in the structure adopted in the solid state, the d_{yz} and d_{xz} orbitals of the Ru atom are able to participate in conjugation along the carbon-rich bridging ligand. The octa-1,3,5,7-tetrayn-1,8-diyl ligand in **6**•$2CH_2Cl_2$ displays the sigmoidal distortions from linearity often observed for extended carbon chain complexes.[82,84] In **5**•CH_2Cl_2 the Ru-C(1) distance (1.965(10) Å) is the shortest in the series, and arguably shorter than the Ru-C_α bond found in the related hexa-1,3,5-triyne-1,6-diyl complex [{$Ru(PPh_3)_2Cp$}$_2$(μ-C≡CC≡CC≡C)] (2.001(6) Å),[77] and in **6**•$2CH_2Cl_2$, but equal to that found in **6**•$4CHCl_3$ (1.963(6) Å).[82] Clearly, these small structural variations must be treated cautiously to avoid over-interpretation.

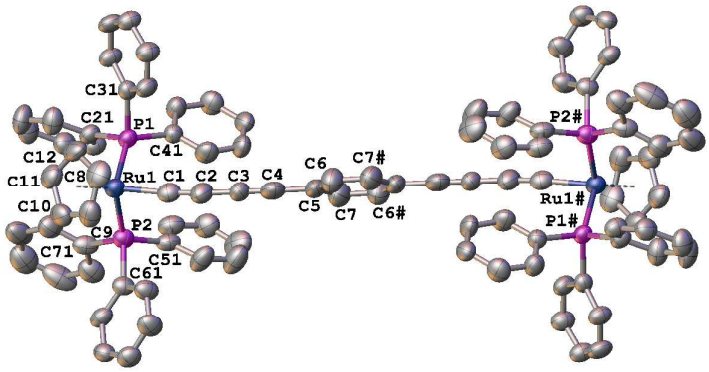

Fig. 2. A plot of a molecule of **5**•CH_2Cl_2. The molecule is located in the center of symmetry.

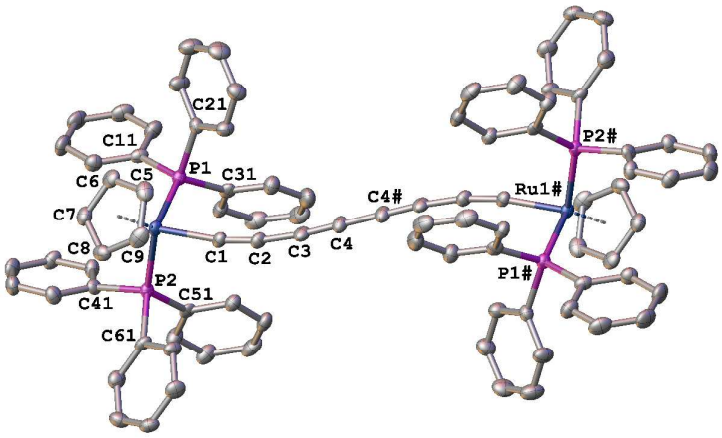

Fig. 3. A plot of a molecule of **6**•2CH_2Cl_2. The molecule is located in the center of symmetry.

Electrochemistry

The monometallic complexes **4a**-**4e** each give one oxidation wave that is electrochemically reversiblebut chemically irreversible, supported by the observation of a 30 mV shift in the peak potential per decade change in scan rate, and peak currents linear vs $\nu^{1/2}$, with peak potentials at 100 mV/s that vary between 0.06 V-0.22 V and exhibit a trend in accord with the electronic character of the aryl substituent: Ru(C≡CC≡CC_6H_4OMe-4)$(PPh_3)_2$Cp **4c** < Ru(C≡CC≡CC_6H_4Me-4)$(PPh_3)_2$Cp **4b** < Ru(C≡CC≡CDHBT)$(PPh_3)_2$Cp **4d** < Ru(C≡CC≡CC_6H_4CN-4)$(PPh_3)_2$Cp **4a** < Ru(C≡CC≡CC_5H_4N)$(PPh_3)_2$Cp **4e** (Table 2). The irreversibility of similar diynyl complexes has been noted on previous occasions,[18] and is likely due to intermolecular coupling of the generated diynyl radicals.[66,85] A general scheme on this oxidation dimerization process is depicted in Scheme 2.

Table 2. Electrochemical data of the Ru(C≡CC≡C-Ar)$(PPh_3)_2$Cp derivatives **4a-e**, **5**, and **6**.[a]

Compound	$E_{pa}(1)$	$E_{pa}(2)$	$E_{pa}(3)$	$E_{pa}(4)$
Ru(C≡CC≡CC_6H_4OMe-4)$(PPh_3)_2$Cp **4c**	0.06			
Ru(C≡CC≡CC_6H_4Me-4)$(PPh_3)_2$Cp **4b**	0.09			
Ru(C≡CC≡CDHBT)$(PPh_3)_2$Cp **4d**	0.11			
Ru(C≡CC≡CC_6H_4CN-4)$(PPh_3)_2$Cp **4a**	0.21			
Ru(C≡CC≡CC_5H_4N)$(PPh_3)_2$Cp **4e**	0.22			
{Ru$(PPh_3)_2$Cp}$_2$(μ-C≡CC≡CC_6H_5C≡CC≡C) **5**	0.04	0.24		
	$E_{1/2}(1)$	$E_{pa}(2)$	$E_{pa}(3)$	$E_{pa}(4)$
{Ru$(PPh_3)_2$Cp}$_2$(μ-C≡CC≡CC≡CC≡C) **6**	-0.16	0.15	0.61	0.82

[a] E_{pa} (anodic peak potential, V) vs. ferrocene/ferrocenium ($FeCp_2/[FeCp_2]^+$ = 0 V) (CH_2Cl_2, 0.1 M NBu_4PF_6, Pt dot working electrode). Data recorded against an internal decamethylferrocene/ decamethylferrocenium ($FeCp^*_2/[FeCp^*_2]^+$) standard. Under these conditions $FeCp^*_2/[FeCp^*_2]^+$ = -0.53 V vs $FeCp_2/[FeCp_2]^+$.

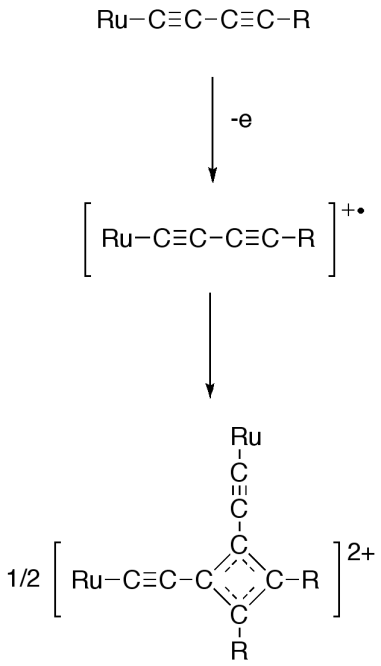

Scheme 2. A general oxidation and dimerization process for a Ru-C≡C-C≡C-R complex [Ru = Ru(PP)Cp´ where PP = $(PPh_3)_2$ or dppe, Cp´ = Cp or Cp*; R = aryl or -$(C\equiv C)_n$-Ru].

Similarly, two electrochemically reversible, but chemically irreversible, oxidation waves (peak potential displaying 30 mV shift per decade change in scan rate, peak currents linear vs $\nu^{1/2}$) are observed in the cyclic voltammogram of the bis(butadiynyl) complex **5** (Table 2). The chemical stability of $[\mathbf{5}]^+$ did not improve at lower temperatures (ambient to -30 °C) and chemical complications evidenced by the appearance of a new reduction wave at -0.15 V on the return scan were still apparent at ν = 800 mV s^{-1}. The chemical instability of this bis(butadiynyl) complex is entirely consistent with the limited chemical stability of **4a** – **4e**, and other related systems reported elsewhere.[85]

In contrast to these monometallic buta-1,3-diynyl derivatives, the bimetallic octa-1,3,5,7-tetrayndiyl complex **6** displays one fully reversible oxidation wave (i_{pa}/i_{pc} = 0.98, ΔE_p = 74 mV which is comparable with the internal decamethylferrocene reference) and three subsequent, irreversible processes (Table 2). These four processes correspond well to the four oxidation processes described for the analogous buta-1,3-diyndiyl (-C≡CC≡C-) complex $\{Ru(PPh_3)_2Cp\}_2(\mu\text{-}C{\equiv}CC{\equiv}C)$.[86,87] In the case of the shorter chain analogue, $\{Ru(PPh_3)_2Cp\}_2(\mu\text{-}C{\equiv}CC{\equiv}C)$, the first three redox processes at least are chemically reversible. Spectroelectrochemical studies supported by quantum chemical calculations have been used to demonstrate the progressive shift in the character of the carbon chain from butadiyndiyl (-C≡CC≡C-) through butatrienylidene (=C=C=C=C=) towards butynediyldiide (≡CC≡CC≡).[86,87] The cation $[\{Ru(PPh_3)_2Cp\}_2(\mu\text{-}C{\equiv}CC{\equiv}C)]^+$ is sufficiently kinetically and thermodynamically stable to be isolated, and has been explored in a number of contexts.[86,87] The closely related hexa-1,3,5-triyn-1,6-diyl complex $\{Ru(dppe)_2Cp\}_2(\mu\text{-}C{\equiv}CC{\equiv}CC{\equiv}C)$ exhibits three redox processes in the potential window explored, the first two of which were reversible, the third being only partially chemically reversible.[68] However, in contrast to the C_4 example, the more exposed C_6 chain in $[\{Ru(dppe)_2Cp\}_2(\mu\text{-}C{\equiv}CC{\equiv}CC{\equiv}C)]^+$ undergoes an intermolecular coupling reaction on timescales longer than the voltammetric measurement at temperatures above –10 °C to give an unusual dimeric complex featuring a cyclobutene motif formed by coupling between $C_\alpha{\equiv}C_\beta$ of one molecule with $C_\gamma{\equiv}C_\delta$ of another (Scheme 3).[68] This contrasting reactivity prompted further investigation of the first electrochemically reversible process observed for the C_8 bridged complex **6** by spectroelectrochemical methods.

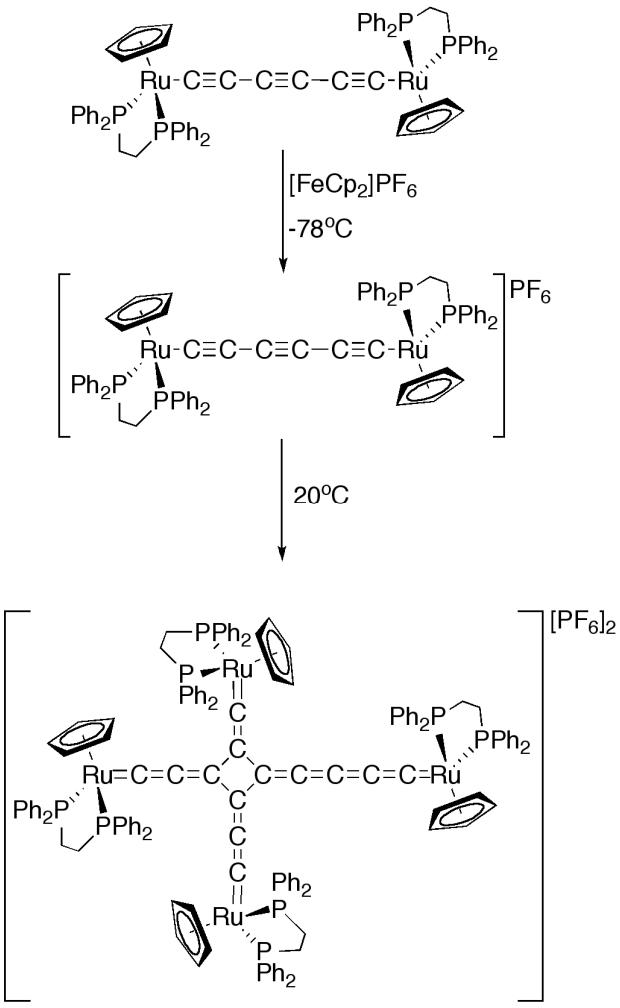

Scheme 3. The synthesis and dimerization of $[\{Ru(dppe)_2Cp\}_2(\mu\text{-}C{\equiv}CC{\equiv}CC{\equiv}C)]^+$.[68]

Spectroelectrochemistry

Spectroelectrochemical (UV-vis-NIR, IR) studies of **6** were conducted in a Hartl-style OTTLE cell[88] in 0.1 M NBu_4PF_6 / CH_2Cl_2 solution at ambient temperature. The characteristic ν(C≡C) bands of **6** were observed at 2107 and 1955 cm^{-1} in the IR spectrum. On oxidation of **6,** the spectrum evolved into a more complex series of ν(CC) bands between 2059 - 1862 cm^{-1} with clear maxima at 2059 s, 2039 sh, 1953 m and 1862 vs cm^{-1} (Figure 4). However, back reduction failed to completely recover

the original spectrum of **6** suggesting an EC process on the longer timescale of the electrolysis, albeit low volume, required for the spectroelectrochemical method.

As noted above, the oxidation of a related hexa-1,3,5-triyn-1,6-diyl complex [{Ru(dppe)Cp}$_2$(μ-C≡CC≡CC≡C)] was reported[68] to give the dimerization product {*cyclo*-C([Ru])C(CCCC[Ru])C(CC]Ru]C(CC[Ru])}$^{2+}$ ([Ru] = Ru(dppe)Cp) (Scheme 3). This dimer has a remarkably similar ν(C≡C) band pattern at 2080 - 1930 cm^{-1} as for the oxidized product shown in Figure 4 and suggests that a dimerization product is also formed on oxidation of **6**.

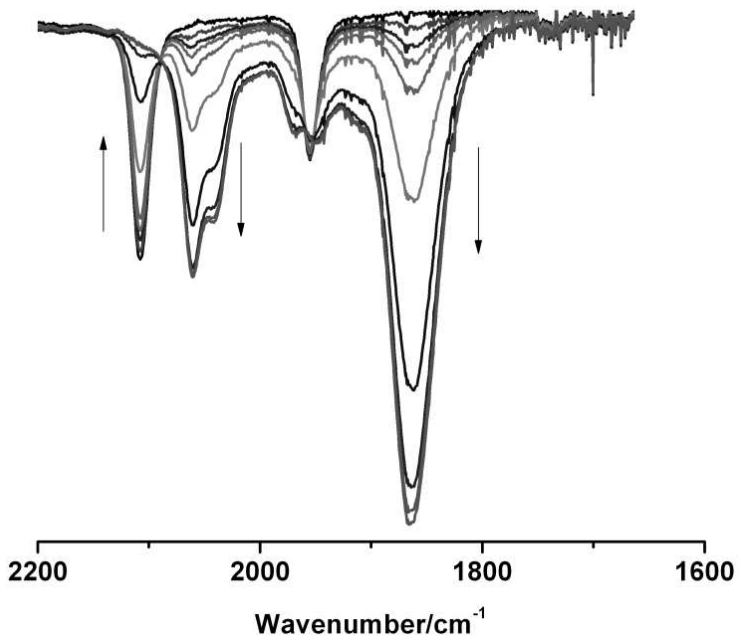

Fig. 4. The IR spectra collected in a spectroelectrochemical cell during oxidation of **6** (0.1 M NBu_4PF_6 / CH_2Cl_2).

The oxidation of **6** was also followed in the UV-vis-NIR region. Upon one-electron oxidation, the spectra display a loss of the intense UV band at 29793 cm^{-1} and the

appearance of new features in the NIR region at 7500 cm^{-1}, which grew and decayed during the earlier stages of the electrolysis, and two further bands at 11048 and 14280 cm^{-1}, which continued to grow throughout the experiment (Figure 5). Again, back-reduction failed to regenerate **6**, confirming the EC process in the initial stages of the spectroelectrochemical experiment.

Although we have not identified the product ultimately formed on oxidation of **6**, the transient band observed at 7500 cm^{-1} likely arises from the initial oxidation product $[\mathbf{6}]^+$, whilst the relatively intense, persistent features observed at the later stages at 11048 and 14280 cm^{-1} are similar to those observed in the absorption spectrum of $\{$*cyclo*-C([Ru])C(CCCC[Ru])C(CC]Ru]C(CC[Ru])$\}^{2+}$ (12060, 16640 cm^{-1}, [Ru] = Ru(dppe)Cp, Scheme 3).[68] It therefore appears probable that the initial oxidation of **6** to give the radical cation $[\mathbf{6}]^+$ is followed by a cyclodimerization process analogous to that observed for oxidation of $[\{Ru(dppe)Cp\}_2(\mu\text{-}C{\equiv}CC{\equiv}CC{\equiv}C)]^+$.

While the radical cation $[\mathbf{6}]^+$ is observed in the UV-vis-NIR spectra on oxidation, the IR bands corresponding to $[\mathbf{6}]^+$ were not observed in the IR spectra on oxidation. The sample concentration used for IR spectroelectrochemistry is higher than for UV-vis-NIR spectroelectrochemistry so the rate of dimerization on oxidation would likely be faster and may account for the failure to detect any appreciable accumulation of $[\mathbf{6}]^+$ in the IR experiments. Given the ample evidence for the highly reactive nature of $[\mathbf{6}]^+$, efforts to isolate this species were not undertaken.

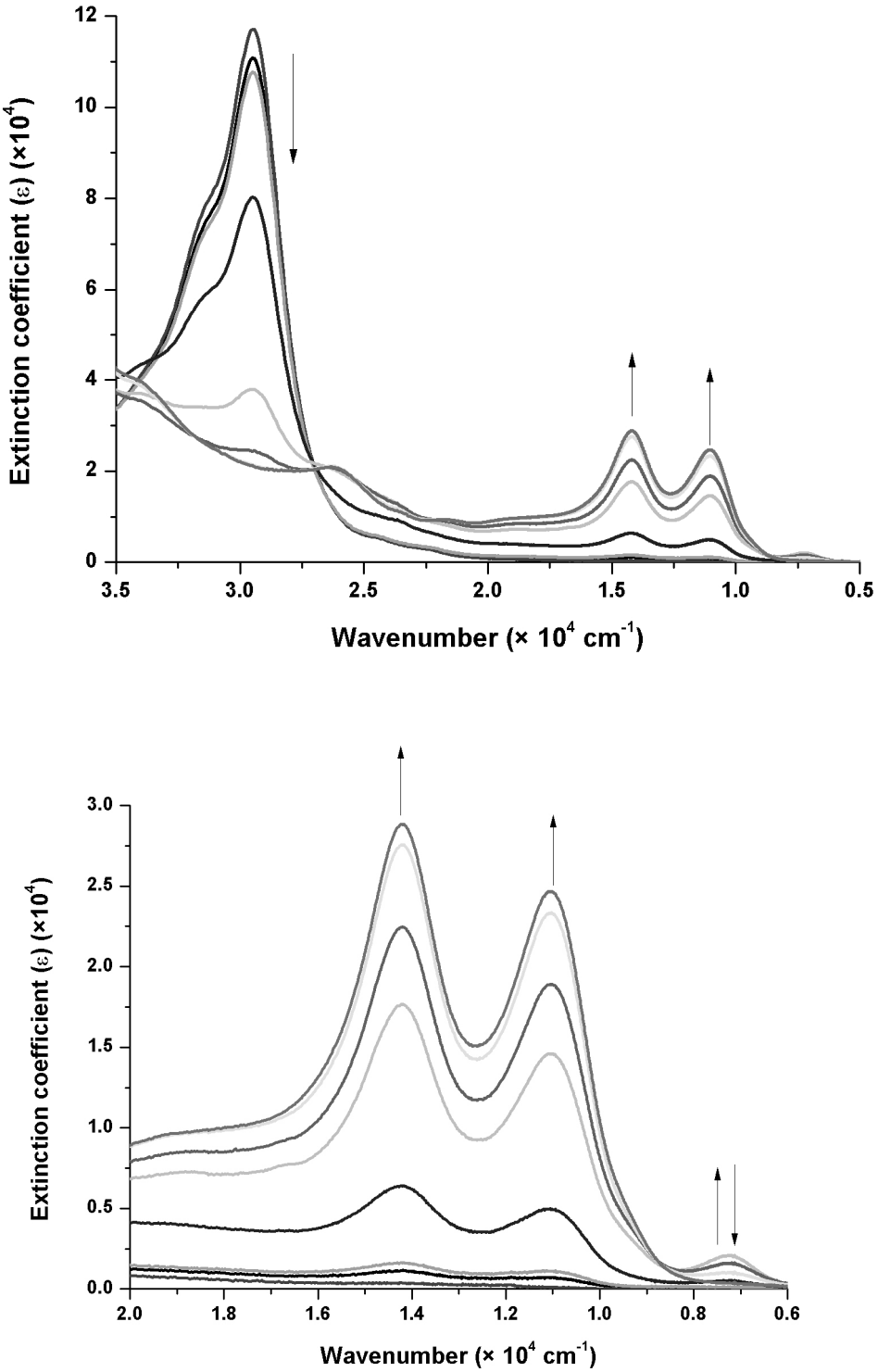

Fig 5. The UV-Vis-NIR spectra collected in a spectroelectrochemical cell during oxidation of **6** (0.1 M NBu_4PF_6 / CH_2Cl_2).

Quantum chemical calculations

The electronic structure of monometallic polyynyl[8,89,90] and bimetallic polyyndiyl[37-39, 87,91] complexes has been explored in detail over the last 20 years at increasingly sophisticated levels of theory. Here, hybrid-DFT calculations (B3LYP/3-21G*/CPCM-CH_2Cl_2) were carried out on the compounds **5** and **6** to investigate the influence of the interpolated phenylene ring on the electronic structure of these π-extended, carbon-rich complexes. The compound **4a** was also studied to aid the assignment of ^{13}C NMR spectra in the series **4a** – **e**. Each system was fully optimized without symmetry constraints, with frequency calculations indicating each structure to be a true minimum. The resulting computational systems are denoted **4a´**, **5´** and **6´** to distinguish them from the physical complexes.

Each structure in the bimetallic complexes adopts mutual *trans*-arrangement of the Cp rings and, in the case of **5´,** the phenylene ring essentially bisects the P-Ru-P angles at each metal (Cp(0)-Ru(1)-C(5)-C(7): –172.9° (**5**); 165.26 (**5´**): Cp(0) is the centroid of the Cp ring). The selected bond lengths and angles for **4a´, 5´** and **6´** summarized in Table 1 enable comparison with the crystallographically determined structures. The majority of experimental bond lengths are reproduced well with differences of < 0.02 Å. The most significant deviations arise from the Ru-P distances in **6**, which are over-estimated by 0.04 - 0.06 Å, and the ±0.06 Å difference between the calculated C(3)-C(4) and C(4)-C(5) distances in **5´** and the values obtained from the relatively low precision crystallographic structure. Nevertheless, deviations of this magnitude are

not uncommon for calculations of organometallic complexes and the overall level of agreement is more than satisfactory.

The electronic structures of **5´** (Table 3) and **6´** (Table 4) were also examined, those of buta-1,3-diynyl complexes having been well discussed elsewhere,[8,89,90] and give features that are broadly as expected for half-sandwich alkynyl-derivatives.[92-94] Thus, in each case the HOMO and HOMO–1 have dπ/π character along the Ru-C≡C-…-C≡C-Ru backbone, with the usual nodal planes between the formally singly-bonded atoms (Figure 6).

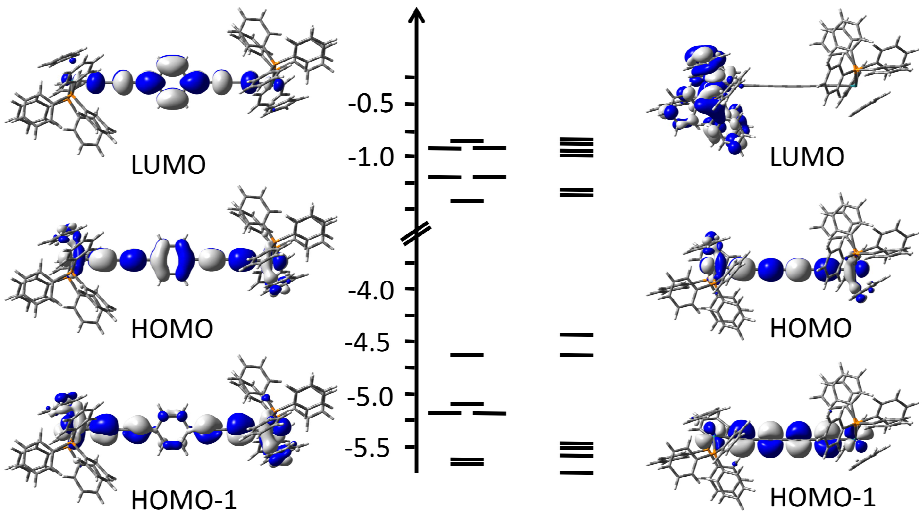

Figure 6. MO diagrams of **5´** (left) and **6´** (right) and plots of key frontier molecular orbitals (contour value ±0.02 $(e/bohr^3)^{1/2}$).

These filled frontier orbitals are well separated from the LUMO and LUMO+1 ($\Delta E_{HOMO\text{-}LUMO}$: 3.31 eV (**5´**), 3.20 eV (**6´**)), which in **6´** are essentially degenerate, and largely located on the $Ru(PPh_3)_2Cp$ fragments. However, at this level of theory, in **5´** the LUMO is bis(butadiynyl)benzene π* orbital in character, with the degenerate $Ru(PPh_3)_2Cp$ metal-ligand anti-bonding orbitals forming the LUMO+1 and LUMO+2 and lying ca. 0.1 eV above the LUMO.

Whilst the dπ/π-type HOMO of **5´** is delocalized extensively along the entire length of the $RuC{\equiv}CC{\equiv}CC_6H_4C{\equiv}CC{\equiv}CRu$ chain (ca. 24% Ru, 48% C_4, 15% C_6H_4), the planar phenylene moiety breaks the conjugation in the orthogonal HOMO–1 (ca. 38% Ru, 40% C_4, 4% C_6H_4), and gives a substantial HOMO to HOMO–1 gap of ca. 0.5 eV. In contrast, the cylindrical symmetry of the all-carbon chain in **6´** results in a more similar composition and energy of the HOMO (–4.46 eV; 27% Ru, 62% C_8) and HOMO–1 (–4.64 eV; 27% Ru, 67% C_8). The presence of one (**5´**) or two (**6´**) occupied orbitals in the frontier region is consistent with the observation of two (**5´**) or four (**6´**) oxidation processes in these complexes. In addition, the lower lying HOMO of **5´** is consistent with the more positive redox potentials (Table 2) observed for the first and second processes of **5´** relative to **6´**.

Table 3. Orbital energies (eV) and composition (%) for selected frontier orbitals of **5′**.

MO		eV	Cp1	$PPh_3$1	Ru1	Cα1	Cβ1	Cγ1	Cδ1	C_6H_4	Cδ2	Cχ2	Cβ2	Cα2	Ru2	$PPh_3$2	Cp2
405	L+5	-0.81	4	76	10	1	0	0	0	0	0	0	0	0	1	8	0
404	L+4	-0.85	1	98	1	0	0	0	0	0	0	0	0	0	0	0	0
403	L+3	-0.85	0	0	0	0	0	0	0	0	0	0	0	0	1	98	1
402	L+2	-1.23	0	0	0	0	0	0	0	0	0	0	0	0	32	54	14
401	L+1	-1.23	14	54	32	0	0	0	0	0	0	0	0	0	0	0	0
400	LUMO	-1.33	1	1	2	8	0	11	3	49	3	11	0	8	2	1	1
399	HOMO	-4.64	3	3	12	5	8	4	7	15	7	4	8	5	12	3	3
398	H-1	-5.14	5	4	20	3	10	1	7	4	6	1	9	3	18	4	5
397	H-2	-5.2	1	1	6	1	3	0	2	2	11	2	15	6	40	5	5
396	H-3	-5.2	5	5	40	6	15	2	11	2	2	0	3	1	7	1	1
395	H-4	-5.61	19	16	34	5	4	1	4	1	1	0	1	1	6	3	4
394	H-5	-5.62	4	3	6	1	1	0	1	1	4	1	5	5	33	16	19

Table 4. Orbital energies (eV) and composition (%) for selected frontier orbitals of **6′**.

MO		eV	Cp1	$PPh_3$1	Ru1	Cα1	Cβ1	Cχ1	Cδ1	Cδ2	Cχ2	Cβ2	Cα2	Ru2	$PPh_3$2	Cp2
385	L+5	-0.81	2	31	6	7	0	8	4	4	8	0	7	6	13	3
384	L+4	-0.82	2	60	9	4	0	4	2	2	4	0	3	2	6	1
383	L+3	-0.88	1	68	2	3	0	3	2	2	3	0	3	3	8	1
382	L+2	-0.9	0	3	0	1	0	1	1	1	1	0	1	6	82	2
381	L+1	-1.25	0	0	0	0	0	0	0	0	0	0	0	34	52	15
380	LUMO	-1.26	15	53	32	0	0	0	0	0	0	0	0	0	0	0
379	HOMO	-4.46	3	3	13	8	8	7	7	8	7	9	8	14	3	3
378	H-1	-4.64	1	1	14	9	8	8	8	8	9	8	9	13	1	1
377	H-2	-5.44	7	6	21	0	8	1	4	4	1	8	0	25	6	8
376	H-3	-5.46	13	10	34	1	2	0	1	1	0	3	1	21	6	7
375	H-4	-5.56	10	7	18	2	1	1	1	1	1	1	2	27	14	17
374	H-5	-5.88	4	7	28	1	8	0	4	4	0	8	1	23	6	4

Conclusion

We have demonstrated that the availability of stable terminal buta-1,3-diynyl complexes makes Sonogashira cross-coupling protocols an appealing entry point for the preparation of a wide range of substituted buta-1,3-diynyl compounds, thereby avoiding the preparation of buta-1,3-diyne ligand precursors. The process is suitable for the preparation of 'simple' buta-1,3-diynyl complexes, i.e. those bearing substituents, which are chemically and functionally rather complex, such as 2,3-dihydrobenzo[*b*]thiophene (**4d**) and pyridine (**4e**), and more elaborate bis(diynyl) complexes such as **5**. Facile homo-coupling of Ru(C≡CC≡CH)$(PPh_3)_2$Cp in the presence of Pd(II) / Cu(I) co-catalysts and air as an oxidant affords the octa-1,3,5,7-tetra-1,8-diyl complex **6**. Whilst the chemical reactivity of $[\mathbf{5}]^+$ and $[\mathbf{6}]^+$ prevented detailed analysis of these compounds by spectroelectrochemical methods, DFT calculations indicate the significant organic character in the frontier orbitals of **5´** and **6´**. The significant difference in the relative energy and composition of the HOMO-1 in these complexes is consistent with the trends in electrochemical properties. The work described here therefore extends the 'chemistry on the complex' approach to the preparation of complex organometallic compounds, and further illustrates the facile synthetic routes that may be developed using this strategy.

Experimental

General conditions. All reactions were carried out in oven-dried glassware under oxygen-free argon atmosphere using standard Schlenk techniques. Diisopropylamine and triethylamine were purified by distillation from KOH, other reaction solvents were purified and dried using Innovative Technology SPS-400 and degassed before

use. The compounds $Ru(C{\equiv}CC{\equiv}CH)(PPh_3)_2Cp$[18] and **3d**[95] were prepared by literature methods. Other reagents were purchased commercially and used as received. NMR spectra were recorded in deuterated solvent solutions on Bruker Avance 400 MHz and Varian VNMRS 700 MHz spectrometers and referenced against residual protio-solvent resonances ($CHCl_3$: ^{1}H 7.26 ppm, ^{13}C 77.00 ppm and CH_2Cl_2: ^{1}H 5.32 ppm, ^{13}C 53.84 ppm). In the NMR peak assignments, the phenyl ring associated with the dppe and PPh_3 are denoted Ph, and Ar indicates any arylene group belonging to the alkynyl ligands. NMR spectra for **4a-e**, **5** and **6** are depicted in Figures S1-S28. The C_β, C_γ and C_δ ^{13}C NMR peaks were assigned with the aid of computed GIAO-NMR data and are listed in Table S1.

Matrix-assisted laser desorption ionization (MALDI) mass spectra were recorded using an Autoflex II TOF/TOF mass spectrometer with a 337 nm laser. Infrared spectra were recorded on a Thermo 6700 spectrometer from CH_2Cl_2 solution in a cell fitted with CaF_2 windows. Electrochemical analyses were recorded using a BAS CV50W electrochemical analyzer fitted with a three-electrode system consisting of a Pt disk as working electrode, auxiliary and reference electrode from solution in CH_2Cl_2 containing 0.1 M NBu_4PF_6. Plots of the CVs of **4a-e**, **5** and **6** are shown in Figures S29-S32.

X-ray crystallography. Single-crystal X-ray data for compounds **4a,b,d** were collected at 120(2) K on a Bruker SMART CCD 6000 (fine-focus sealed tube, graphite-monochromator) and for compound **6** on a Bruker D8Venture (Photon 100 CMOS detector, IμS microsource, focusing mirrors) diffractometers using Mo Kα

radiation (λ = 0.71073 Å). The data for extremely small and weakly diffracting crystals of **5** were collected at 150(2) K on a Rigaku Saturn 724+ diffractometer at station I19 of the Diamond Light Source (UK) synchrotron (undulator, λ = 0.6889 Å, ω-scan, 1.0°/frame). The temperature on the crystals was maintained with Cryostream (Oxford Cryosystems) open-flow nitrogen cooling devices. All structures were solved by direct methods and refined by full-matrix least squares on F^2 for all data using SHELXL[96] and OLEX2[97] software. All non-disordered non-hydrogen atoms were refined with anisotropic displacement parameters; H atoms were placed in the calculated positions and refined in riding mode. One of the Cl atoms in the CH_2Cl_2 solvate molecule in the structure **6** showed abnormal a.d.p.'s and was modelled as disordered over two positions with fixed SOF 0.8 and 0.2. The largest component was refined in anisotropic mode, the minor one was left isotropic. The attempts to model a possible disorder of corresponding carbon atom did not result in any improvement of the model and the atom was refined with full occupancy. Crystallographic data for the structures have been deposited with the Cambridge Crystallographic Data Centre as supplementary publications CCDC-1033080-1033084.

General procedure for the preparation of the buta-1,3-diynyl ruthenium (II) complexes ***4a*** ***4b****,* ***4c****,* ***4d****,* ***4e****:* In a Schlenk flask, a mixture of $Ru(C{\equiv}CC{\equiv}CH)(PPh_3)_2Cp$ (**2**), 1.5 equivalents of the appropriate iodoaryl, 5%-mol $Pd(PPh_3)_4$ and 10%-mol CuI was added to degassed diisopropylamine ($NHPr^i_2$) (1mL/mmol). The reaction mixture was heated at 90 °C for 2 h after which time the heating bath was removed and the solution allowed to cool to room temperature. The resulting precipitate was collected by filtration, washed with cold hexane, dried, and washed with cold MeOH, and dried in air to give the final compound.

Ru(C≡CC≡C-C$_6$H$_4$CN-4)(PPh$_3$)$_2$Cp (***4a***).[98] From **2** (100 mg, 0.135 mmol) and isolated as a honey-yellow colored solid. Yield: 53 mg, 0.063 mmol (47%). Single crystals suitable for X-ray diffraction were grown by slow diffusion of methanol into a CH_2Cl_2 solution containing 5% NEt_3. ^{1}H NMR (400 MHz, $CDCl_3$): δ 7.43 (ABq, J = 8.2 Hz, 4H, Ar), 7.37-7.35 (m, 12H, Ph), 7.21-7.19 (m, 6H, Ph), 7.12-7.10 (m, 12H, Ph), 4.33 (s, 5H, Cp) ppm. ^{31}P {^{1}H} NMR (162 MHz, $CDCl_3$): δ 48.2 (s) ppm. ^{13}C{^{1}H} NMR (700 MHz, $CDCl_3$): δ 138.1-137.8 (m, Ph_i), 134.1 (t, J = 24.7 Hz, C_α) 133.6 (t, J = 4.9 Hz, Ph_o), 132.6 (HC_{Ar}), 131.6 (C_{Ar}), 131.5 (HC_{Ar}), 128.7 (Ph_p), 127.4 (t, J = 4.6 Hz, Ph_m), 119.3 (*C*≡N), 108.2 (C_{Ar}), 96.0 (C_β), 85.9 (Cp), 85.7 (C_γ), 61.8 (C_δ) ppm. IR (CH_2Cl_2): ν(C≡CC≡C) 2147 s, 2017 m cm^{-1}. MS (MALDI-TOF): *m/z* 579.2 [M-PPh$_3$]$^+$, 719 [Ru(CO)(PPh$_3$)$_2$Cp]$^+$, 841 [M]$^+$. HR-ESI$^+$-MS: *m/z* calcd for $C_{52}H_{40}NP_2{}^{96}Ru$ 836.1712; found 836.1737. *Crystal data for* ***4a***: $C_{52}H_{39}NP_2Ru$, M = 840.85, monoclinic, space group $P2_1/c$, a = 14.2477(6), b = 16.6875(8), c = 17.3130(8) Å, β = 90.515(1)°, U = 4116.1(3) Å^3, F(000) = 1728, Z = 4, Dc = 1.357 mg m^{-3}, μ = 0.496 mm^{-1}. 64895 reflections were collected yielding 10431 unique data (Rmerg = 0.0691). Final $wR_2(F^2)$ = 0.0818 for all data (505 refined parameters), conventional R1(F) = 0.0330 for 7972 reflections with $I \geq 2\sigma$, GOF = 1.007.

Ru(C≡CC≡C-C$_6$H$_4$CH$_3$-4)(PPh$_3$)$_2$Cp (***4b***). From **2** (40 mg, 0.054 mmol) to give a yellow solid. Yield: 39 mg, 0.047 mmol (87%). Single crystals suitable for X-ray diffraction were grown by slow diffusion of methanol into a CH_2Cl_2 solution containing 5% NEt_3. ^{1}H NMR (400 MHz, $CDCl_3$): δ 7.44-7.39 (m, 12H, Ph), 7.34-7.32 (m, 2H, Ar), 7.26-7.20 (m, 6H, Ph), 7.15-7.11(m, 12H, Ph), 7.05-7.03 (m, 2H,

Ar), 4.33 (s, 5H, Cp), 2.32 (s, 3H, CH_3) ppm. $^{31}P\{^1H\}$ NMR (162 MHz, $CDCl_3$): δ 48.4 (s) ppm. $^{13}C\{^1H\}$ NMR (700 MHz, $CDCl_3$): δ 138.3-137.8 (m) (Ph_i), 135.5 (C_{Ar}), 133.6 (t, J = 5.1 Hz, Ph_o), 132.0 (HC_{Ar}), 128.4, 128.3 (HC_{Ar} or Ph_p), 127.1 (t, J = 4.6 Hz, Ph_m), 122.8 (t, J = 24.9 Hz, C_α), 122.7 (C_{Ar}), 95.4 (C_β), 85.4 (Cp), 79.3 (C_γ), 62.7 (C_δ), 21.1 (CH_3) ppm. IR (CH_2Cl_2): ν(C≡CC≡C) 2159 s, 2021 m cm^{-1}. MS (MALDI-TOF): *m/z* 568.2 $[M\text{-}PPh_3]^+$, 830.0 $[M]^+$. HR-ESI$^+$-MS: *m/z* calcd for $C_{52}H_{42}P_2{}^{96}Ru$ 824.1838; found 824.1862. *Crystal data for* ***4b***: $C_{52}H_{42}P_2Ru$, M = 829.87, monoclinic, space group $P2_1/n$, a = 12.9342(9), b = 23.3662(17), c = 13.3100(10) Å, β = 98.512(2)°, U = 3978.3(5) $Å^3$, F(000) = 1712, Z = 4, D_c = 1.386 mg m^{-3}, μ = 0.511 mm^{-1}. 45590 reflections were collected yielding 9605 unique data (R_{merg} = 0.0997). Final $wR_2(F^2)$ = 0.0860 for all data (497 refined parameters), conventional $R_1(F)$ = 0.0413 for 5906 reflections with I ≥ 2σ, GOF = 0.961.

*Ru(C≡CC≡C-C_6H_4OMe-4)(PPh_3)$_2$Cp (**4c**).* From **2** (40 mg, 0.054 mmol) to give a yellow solid. Yield: 27 mg, 0.032 mmol (59%). ^1H NMR (400 MHz, $CDCl_3$): δ 7.43-7.40 (m, 12H, Ph), 7.37 (d, J = 8.6 Hz, 2H, Ar), 7.24-7.20 (m, 6H, Ph), 7.15-7.11 (m, 12H, Ph), 6.79 (d, J =8.6 Hz, 2H, Ar), 4.33 (s, 5H, Cp), 3.80 (s, 3H, OMe) ppm. $^{31}P\{^1H\}$ NMR (162 MHz, $CDCl_3$): δ 49.1(s) ppm. $^{13}C\{^1H\}$ NMR (600 MHz, $CDCl_3$): δ 158.0 (C_{Ar}-OMe), 138.6-137.9 (m, Ph_i), 133.7 (t, J = 5.1 Hz, Ph_o), 133.5 (HC_{Ar}), 128.5 (Ph_p), 127.3 (t, J = 4.7 Hz, Ph_m), 122.1 (t, J = 25.0 Hz, C_α), 118.1 (C_{Ar}), 113.6 (HC_{Ar}), 95.4 (C_β), 85.6 (Cp), 78.7 (C_γ), 62.4 (C_δ), 55.1 (O-CH_3). IR (CH_2Cl_2): ν(C≡CC≡C) 2160, 2021 cm^{-1}. MS (MALDI-TOF): *m/z* 584.1 $[M\text{-}PPh_3]^+$, 846.1 $[M]^+$. HR-ESI$^+$-MS: *m/z* calcd for $C_{52}H_{42}OP_2{}^{96}Ru$ 840.1787; found 840.1828.

*Ru(C≡C-C≡C-DHBT)(PPh$_3$)$_2$Cp (**4d**)*. From **2** (40 mg, 0.054 mmol) to give a mustard-colored solid. Yield: 25 mg, 0.029 mmol (54%). Single crystals suitable for X-ray diffraction were grown by slow diffusion of methanol into a CH_2Cl_2 solution containing 5% NEt_3. ^{1}H NMR (400 MHz, $CDCl_3$): δ 7.42-7.37 (m, 12H, Ph), 7.24-7.18 (m, 8H, Ph + Ar), 7.13-7.09 (m, 12H, Ph), 7.06 (d, J = 8.0 Hz, 1H, Ar), 4.32 (s, 5H, Cp), 3.35-3.31 (m, 2H), 3.24-3.20 (m, 2H) ppm. ^{31}P {^{1}H} NMR (162 MHz, $CDCl_3$): δ 48.4 (s) ppm. ^{13}C{^{1}H} NMR (700 MHz, $CDCl_3$): δ 139.8 (C_{Ar}), 139.3 (C_{Ar}), 138.3-138.1 (m, Ph_i), 133.7 (t, J = 4.9 Hz, Ph_o), 131.5 (HC_{Ar}), 128.5 (Ph), 128.0 (HC_{Ar}), 127.3 (t, J = 4.6 Hz, Ph_m), 121.6 (C_{Ar}), 121.5 (HC_{Ar}), 95.5 (C_β), 85.6 (Cp), 79.7 (C_γ), 62.7 (C_δ), 35.9 (CH$_2$), 33.4 (CH$_2$) ppm, the C_α peak was not visible. IR (CH_2Cl_2): ν(C≡CC≡C) 2156, 2015 cm^{-1}. MS (MALDI-TOF): *m/z* 719.1 [Ru(CO)(PPh$_3$)$_2$Cp]$^+$, 875.2 [M]$^+$. HR-ESI$^+$-MS: *m/z* calcd for $C_{53}H_{42}P_2S^{96}Ru$ 868.1558; found 868.1597. *Crystal data for **4d***: $C_{53}H_{42}P_2RuS$, M = 873.94, monoclinic, space group P 2$_1$/n, a = 11.2014(7), b = 16.3616(11), c = 22.0949(14) Å, β = 90.675(2)°, U = 4049.1(5) Å^3, F(000) = 1800, Z = 4, D_c = 1.434 mg m^{-3}, μ = 0.556 mm^{-1}. 66387 reflections were collected yielding 10767 unique data (R_{merg} = 0.0420). Final w$R_2(F^2)$ = 0.0423 for all data (682 refined parameters), conventional $R_1(F)$ = 0.0315 for 8977 reflections with I ≥ 2σ, GOF = 1.065.

*Ru(C≡CC≡C-C$_5$H$_4$N)(PPh$_3$)$_2$Cp (**4e**).* From **2** (50 mg, 0.067 mmol) to give a yellow powder. Yield: 33 mg, 0.040 mmol (60%). ^{1}H NMR (400 MHz, CD_2Cl_2): δ 8.40 (d, J = 6.1 Hz, 2H, Ar), 7.39-7.36 (m, 12H, Ph), 7.29-7.27 (m, 6H, Ph), 7.22 (d, J = 6.1 Hz,

2H, Ar), 7.18-7.15 (m, 12H, Ph), 4.38 (s, 5H, Cp) ppm. $^{31}P\{^1H\}$ NMR (162 MHz, $CDCl_3$): δ 48.9 (s) ppm. $^{13}C\{^1H\}$ NMR (600 MHz, $CDCl_3$): δ 149.0 (HC_{Ar}), 138.1-137.8 (m, Ph_i), 134.6 (C_{Ar}), 133.6 (t, J = 5.0 Hz, Ph_o), 128.7 (Ph_p), 127.4 (t, J = 5.0 Hz, Ph_m), 126.4 (HC_{Ar}), 95.7 (C_β), 85.9 (Cp), 85.7 (C_γ), 60.4 (C_δ), the C_α peak was not visible. IR (CH_2Cl_2): ν(C≡CC≡C) 2150 m, 2006 cm^{-1}. MS (MALDI-TOF): *m/z* 817.1, $[M]^+$. HR-ESI^+-MS: *m/z* calcd for $C_{50}H_{40}NP_2{}^{96}Ru$ 812.1712; found 812.1740.

{Ru(PPh$_3$)$_2$Cp}$_2$(μ-C≡C-C≡CC$_6$H$_5$C≡C-C≡C) (***5***). A solution of Ru(C≡CC≡CH)(PPh_3)$_2$Cp (**2**) (100 mg, 0.135 mmol), 1,4-diiodobenzene (23 mg, 0.067 mmol), $Pd(PPh_3)_4$ (7 mg, 0.006 mmol) and CuI (2 mg, 0.012 mmol) in diisopropylamine (10 mL) was stirred for 2 h at room temperature before being heated at reflux for 2 h. The solvent was removed, and the residue purified on a neutral alumina column eluted with CH_2Cl_2:NEt_3 (95:5 v/v). The yellow band was collected and reduced to the minimum volume prior to addition of MeOH (5 mL). On further concentration, a gold-brown solid precipitated which was collected by filtration, washed with MeOH and air-dried. Yield: 70 mg, 0.045 mmol (67%). Single crystals suitable for X-ray diffraction were grown by slow diffusion of diethyl ether into a CH_2Cl_2 solution containing 5% NEt_3. ^1H NMR (400 MHz, $CDCl_3$): δ 7.44-7.29 (m, 24H, Ph), 7.30 (s, 4H, Ar), 7.25-7.21 (m, 12H, Ph), 7.15-7.12 (m, 24H, Ph), 4.34 (s, 10H, H_{Cp}) ppm. $^{31}P\{^1H\}$ NMR (162 MHz, $CDCl_3$): δ 48.4 (s) ppm. $^{13}C\{^1H\}$ NMR (700 MHz, $CDCl_3$): δ 138.3-138.1 (Ph_i), 133.7 (t, J = 5.0 Hz, Ph_o), 131.8 (HC_{Ar}), 128.5 (Ph_p), 127.3 (t, J = 4.7 Hz), Ph_m), 125.7 (t, J = 23.0 Hz, C_α), 123.4 (C_{Ar}), 95.9 (C_β), 85.6 (Cp), 81.8 (C_γ), 63.4 (C_δ), the C_α peak was not visible. IR (CH_2Cl_2): ν(C≡CC≡C) 2155 s, 2016 m cm^{-1}. MS (MALDI-TOF; *m/z*): 1554.0 $[M]^+$. HR-ESI^+-

MS: *m/z* calcd for $C_{96}H_{74}P_4Ru_2$ 1554.2871; found: 1554.2665. *Crystal data for* ***5***: $C_{96}H_{74}P_4Ru_2.CH_2Cl_2$, M = 1638.50, monoclinic, space group $P2_1/c$, a = 16.693(7), b = 11.384(4), c = 21.646(9) Å, β = 98.678(5)°, U = 4066(3) $Å^3$, F(000) = 1680, Z = 2, D_c = 1.338 mg m^{-3}, μ = 0.563 mm^{-1}. 20671 reflections were collected yielding 6114 unique data (R_{merg} = 0.0929). Final $wR_2(F^2)$ = 0.2575 for all data (487 refined parameters), conventional $R_1(F)$ = 0.0800 for 3957 reflections with $I \geq 2\sigma$, GOF = 1.024. Due to extremely weak diffraction only reflections with $2\Theta \leq 46°$ were used in the refinement.

*{Ru(PPh$_3$)$_2$Cp}$_2$(μ-C≡CC≡CC≡CC≡C) (**6**).* An open flask was charged with a solution of Ru(C≡CC≡CH)(PPh$_3$)$_2$Cp (**2**) (100 mg, 0.135 mmol), Pd(PPh$_3$)$_4$ (6.8 mg, 0.006 mmol) and an excess of CuI (8 mg) in $NHPr^i_2$ (8 mL). The mixture was stirred at room temperature for 1 h after which time the solution had turned yellow and a brown precipitate had formed. The solvent was removed and the residue purified on a neutral alumina column eluted by CH_2Cl_2/5% NEt_3. After precipitation from hexane a bright yellow solid was obtained. Yield: 55 mg, 0.037 mmol (55%). Crystals suitable for X-ray diffraction were obtained from CH_2Cl_2 / Et_2O by slow diffusion. ^{1}H NMR (400 MHz, CD_2Cl_2): δ 7.42-7.38 (m, 24H, Ph), 7.24-7.21 (m, 12H, Ph), 7.15-7.11 (m, 24H, Ph), 4.31 (s, 10H, Cp) ppm. $^{31}P\{^1H\}$ NMR (162 MHz, $CDCl_3$): δ 48.9 (s) ppm. $^{13}C\{^1H\}$ NMR (600 MHz, CD_2Cl_2): δ 138.9-138.3 (Ph_i), 134.1 (t, J = 5.0 Hz, Ph_o), 129.2 (Ph_p), 127.8 (t, J = 4.6 Hz, Ph_m), 119.6 (t, J = 24.9 Hz, C_α), 96.7 (C_β), 86.4 (Cp), 62.6 (C_γ), 51.7 (C_δ). IR (CH_2Cl_2): ν((C≡C)$_4$) 2107 s, 1955 m cm^{-1}. MS^+ (MALDI-TOF): *m/z* 954.1 $[M-2PPh_3]^+$, 1216.1 $[M-PPh_3]^+$, 1478 $[M]^+$. HR-ESI^+-MS: *m/z* calcd for $C_{90}H_{70}P_4Ru_2$ 1478.2556; found 1478.2368. Calculated for

$C_{91}H_{70}P_4Ru_2.0.5CH_2Cl_2$: C, 71.51; H, 4.71. Found: C, 71.85; H, 4.80. *Crystal data for* ***6***: $C_{90}H_{70}P_4Ru_2.2CH_2Cl_2$, M = 1647.33, triclinic, space group P -1, a = 8.8692(4), b = 12.6858(5), c = 17.6885(7) Å, α = 90.25(2), β = 96.49(2), γ = 96.49(2)°, U = 1895.35(14) $Å^3$, F(000) = 842, Z = 1, D_c = 1.443 mg m^{-3}, μ = 0.672 mm^{-1}. 32488 reflections were collected yielding 8724 unique data (R_{merg} = 0.1696). Final $wR_2(F^2)$ = 0.1745 for all data (464 refined parameters), conventional $R_1(F)$ = 0.0753 for 5362 reflections with $I \geq 2\sigma$, GOF = 0.991.

Computations

All hybrid-DFT computations were carried out with the Gaussian 09 package.[99] The geometries of **4a**, **5** and **6** discussed here were optimized at the B3LYP/3-21G* level of theory[100,101] with no symmetry constraints with the polarized solvent continuum model (dichloromethane) applied.[102] These geometries revealed no imaginary frequencies indicating true minima. Electronic structure calculations were also carried out at the B3LYP/3-21G* level of theory. The MO diagrams and orbital contributions were generated with the aid of GaussView 5.0 and GaussSum packages respectively.[103,104] Theoretical ^{13}C NMR chemical shifts obtained at the GIAO[105]-B3LYP/3-21G*//B3LYP/3-21G* level on the optimized geometries were referenced to TMS: $\delta(^{13}C) = 207.1 - \sigma(^{13}C)$.

Acknowledgements The authors thank EPSRC and ARC for funding and are grateful to the Diamond Light Source for an award of instrument time on the Station I19 (MT 6749) and the instrument scientists for support. PJL held an EPSRC Leadership Fellowship and holds an ARC Future Fellowship (FT120100073).

Supporting Information. Plots of ^{1}H, ^{13}C and ^{31}P NMR spectra. Plots of cyclic voltammograms for **4a-4e**, **5** and **6** and of i_{pa} vs $\sqrt{\nu}$ for **4a**-**4e**. Plots of molecules of **4b** and **4d**. Table comparing observed and computed (GIAO/NMR) ^{13}C NMR shifts for C_β, C_γ and C_δ carbons in **4a**, **5** and **6**. CIF files for compounds **4a**, **4b**, **4d**, **5** and **6**. A text file of Cartesian coordinates for **4a´**, **5´** and **6´** in a format for convenient visualization. This material is available free of charge via the Internet at http://pubs.acs.org.

Dedication.

Dedicated to the memory of Professor Michael F. Lappert, one of the true pioneers in synthetic organometallic chemistry and an example to us all.

References

1. Akita, M.; Chung, M.-C.; Sakurai, A.; Sugimoto, S.; Terada, M.; Tanaka, M.; Moro-oka, Y. *Organometallics* **1997**, *16*, 4882-4691.
2. Mohr, W.; Stahl, J.; Hampel, F.; Gladysz, J.A. *Chem. Eur. J.* **2003**, *9*, 3324-3340.
3. Owen, G.R.; Stahl, J.; Hampel, F.; Gladysz, J.A. *Organometallics* **2004**, *23*, 5889-5892.
4. Stahl, J.; Bohling, J.C.; Peters, T.B.; de Quadras, L.; Gladysz, J.A. *Pure Appl. Chem.* **2008**, *80*, 459-474.
5. Bruce, M.I.; Low, P.J.; Ke, M.; Kelly, B.D.; Skelton, B.W.; Smith, M.E.; White, A.H.; Witton, N.B. *Aust. J. Chem.* **2001**, *54*, 453-460.
6. Roberts, R.L.; Puschmann, H.; Howard, J.A.K.; Yamamoto, J.H.; Carty, A.J.; Low, P.J. *Dalton Trans.* **2003**, 1099-1105.
7. Bruce, M.I.; Costuas, K.; Davin, T.; Ellis, B.G.; Halet, J.-F.; Lapinte, C.; Low, P.J.; Smith, M.E.; Skelton, B.W.; Toupet, L.; White, A.H. *Organometallics* **2005**, *24*, 3864-3881.

8. Gendron, F.; Burgun, A.; Skelton, B.W.; White, A.H.; Roisnel, T.; Bruce, M.I.; Halet, J.-F.; Lapinte, C.; Costuas, K. *Organometallics* **2012**, *31*, 6796-6811.
9. Bruce, M.I.; Scoleri, N.; Skelton B.W. *J. Organomet. Chem.* **2011**, *696*, 3473-3482.
10. Bruce, M.I.; Jevric, M.; Skelton, B.W.; Smith, M.E.; White, A.H.; Zaitseva, N.N. *J. Organomet. Chem.* **2006**, *691*, 361-370.
11. Paul, F.; Meyer, W.E.; Toupet, L.; Jiao, H.; Gladysz, J.A.; Lapinte, C. *J. Am. Chem. Soc.* **2000**, *122*, 9405-9414.
12. Bartlett, M.J.; Hill, A.F.; Smith, M.K. *Organometallics* **2005**, *24*, 5795-5798.
13. Moreno, C.; Arnanz, A.; Delgado, S. *Inorg. Chim. Acta* **2001**, *312*, 139-150.
14. Bruce, M.I.; Ellis, B.G.; Skelton, B.W.; White, A.H. *J. Organomet. Chem.* **2000**, *607*, 137-145.
15. Bruce, M.I.; Costuas, K.; Halet, J.F.; Hall, B.C.; Low, P.J.; Nicholson, B.K.; Skelton, B.W.; White, A.H. *J. Chem. Soc., Dalton Trans.* **2002**, 383-398.
16. Bruce, M.I.; Hall, B.C.; Skelton, B.W.; Smith, M.E.; White, A.H. *J. Chem. Soc., Dalton Trans.* **2002**, 995-1001.
17. Bruce, M.I.; Halet, J.-F.; Le Guennic, B.; Skelton, B.W.; Smith, M.E.; White, A.H. *Inorg. Chim. Acta* **2003**, *350*, 175-181.
18. Bruce, M.I.; Ellis, B.G.; Gaudio, M.; Lapinte, C.; Melino, G.; Giovanni, P.; Paul, F.; Skelton, B.W.; Smith, M.E.; Toupet, L.; White, A.H. *Dalton Trans.* **2004**, 1601-1609.
19. Bruce, M.I.; Low, P.J.; Nicholson, B.K.; Skelton, B.W.; Zaitseva, N.N.; Zhao, X.-I. *J. Organomet. Chem.* **2010**, *695*, 1569-1575.
20. Bruce, M.I.; Büschel, S.; Cole, M.L.; Scoleri, N.; Skelton, B.W.; White, A.H.; Zaitseva, N.N. *Inorg. Chim. Acta* **2012**, *382*, 6-12.
21. Bruce, M.I.; Le Guennic, B.; Scoleri, N.; Zaitseva, N.N.; Halet, J.-F. *Organometallics* **2012**, *31*, 4701-4706.
22. Ying, J.-W.; Liu, I.-P.; Xi, B.; Song, Y.; Campana, C.; Zuo, J.-L.; Ren, T. *Angew. Chem. Int. Ed.* **2010**, *49*, 954-957.
23. Bear, J.L.; Han, B.; Wu, Z.; Van Caemelbecke, E.; Kadish, K.M. *Inorg. Chem.* **2001**, *40*, 2275-2281.
24. Falloon, S.B.; Arif, A.M.; Gladysz, J.A. *Chem. Commun.* **1997**, 629-630.

25. Semenov, S.N.; Taghipourian, S.F.; Blacque, O.; Fox, T.; Venkatesan, K.; Berke, H. *J. Am. Chem. Soc.* **2010**, *132*, 7584-7585.
26. Lissel, F.; Fox, T.; Blacque, O.; Polit, W.; Winter, R.F.; Venkatesan, K.; Berke, H. *J. Am. Chem. Soc.* **2013**, *135*, 4051-4060.
27. AlQaiai, S.M.; Galat, K.J.; Chai, M.H.; Ray, D.G.; Rinaldi, P.L.; Tessier, C.A.; Youngs, W.J. *J. Am. Chem. Soc.* **1998**, *120*, 12149-12150.
28. Horn, C.R.; Gladysz, J.A. *Eur. J. Inorg. Chem.* **2003**, 2211-2218.
29. Owen, G.R.; Hampel, F.; Gladysz, J.A. *Organometallics* **2004**, ***23***, 5893-5895.
30. Chisholm, M.H. *Angew. Chem. Int. Ed. Engl.* **1991**, *30*, 673-674.
31. Takahashi, S.; Kariya, M.; Yatake, T.; Sonogashira, K.; Hagihara, N. *Macromol.* **1978**, *11*, 1063-1066.
32. Hagihara, N.; Sonogashira, K.; Takahashi, S. *Adv. Polym. Sci.* **1981**, *41*, 149-179.
33. Fyfe, H.B.; Mlekuz, M.; Zargarian, D.; Taylor, N.J.; Marder, T.B. *J. Chem. Soc., Chem. Commun.* **1991**, 188-190.
34. Marder, T.B.; Lesley, G.; Yuan, Z.; Fyfe, H.B.; Chow, P.; Stringer, G.; Jobe, I.R.; Taylor, N.J.; Williams, I.D.; Kurtz, S.K. *ACS Symp. Ser.* **1991**, *455*, 605-615.
35. Fyfe, H.B.; Mlekuz, M.G.; Taylor, N.J.; Marder, T.B. *NATO ASI Ser., Ser. E,* **2006**, 331-344.
36. Frapper, G.; Kertesz, M. *Inorg. Chem.* **1993**, *32*, 732-740.
37. Belanzoni, P.; Re, N.; Sgamellotti, A.; Floriani, C. *J. Chem. Soc., Dalton Trans.* **1998**, 1825-1835.
38. Zhuravlev, F.; Gladysz, J.A. *Chem. Eur. J.* **2004**, *10*, 6510-6522.
39. Costuas, K.; Rigaut, S. *Dalton Trans.* **2011**, *40*, 5643-5658
40. Moreno, C.; Gómez, J.L.; Medina, R.-M.; Macazaga, M.-J.; Arnanz, A.; Lough, A.; Farrar, D.H.; Delgado, S. *J. Organomet. Chem.* **1999**, *579*, 63-74.
41. Weng, W.; Bartik, T.; Gladysz, J.A. *Angew. Chem. Int. Ed.* **1994**, *33*, 2199-2202
42. Weng, W.; Bartik, T.; Brady, M.; Bartik, B.; Ramsden, J.A.; Arif, A.M.; Gladysz, J.A. *J. Am. Chem. Soc.* **1995**, *117*, 11922-11931
43. Bartik, T.; Weng, W.; Ramsden, J.A.; Szafert, S.; Falloon, S.B.; Arif, A.M.; Gladysz, J.A. *J. Am. Chem. Soc.* **1998**, *120*, 11071-11081.

44. Bruce, M.I.; Scoleri, N.; Skelton, B.W.; White, A.H. *J. Organomet. Chem.* **2010**, *695*, 1561-1568.

45. Wong, A.; Kang, P.C.W.; Tagge, C.D.; Leon, D.R. *Organometallics* **1990**, *9*, 1992-1994.

46. de Quadras, L.; Shelton, A.H.; Kuhn, H.; Hampel, F.; Schanze, K.S.; Gladysz, J.A. *Organometallics* **2008**, *27*, 4979-4991.

47. Bruce, M.I.; Ke, M.; Low, P.J.; Skelton, B.W.; White, A.H. *Organometallics* **1998**, *17*, 3539-3549.

48. Denis, R.; Weyland, T.; Paul, F.; Lapinte, C. *J. Organomet. Chem.* **1997**, *545-546*, 615–618.

49. Le Stang, S.; Lenz, D.; Paul, F.; Lapinte, C. *J. Organomet. Chem.* **1999**, *572*, 189–192.

50. Denis, R.; Toupet, L.; Paul, F.; Lapinte, C. *Organometallics* **2000**, *19*, 4240–4251

51. Courmarcel, J.; Le Gland, G.; Toupet, L.; Paul, F.; Lapinte, C. *J. Organomet. Chem.* **2003**, *670*, 108–122.

52. Hurst, S.K.; Cifuentes, M.P.; McDonagh, A.M.; Humphrey, M.G.; Samoc, M.; Luther-Davies, B.; Asselberghs, I.; Persoons, A. *J. Organomet. Chem.* **2002**, *642*, 259–267.

53. Brady, M.; Weng, W.Q.; Gladysz, J.A. *J. Chem. Soc., Chem. Commun.* **1994**, 2655-2656.

54. Bartik, T.; Bartik, B.; Brady, M.; Dembinski, R.; Gladysz, J.A. *Angew. Chem., Int. Ed.* **1996**, *35*, 414-417.

55. Bartik, B.; Dembinski, R.; Bartik, T.; Arif, A.M.; Gladysz, J.A. *New. J. Chem.* **1997**, *21*, 739-750.

56. Dembinski, R.; Lis, T.; Szafert, S.; Mayne, C.L.; Bartik, T.; Gladysz, J.A. *J. Organomet. Chem.* **1999**, *578*, 229-246.

57. Peters, T.B.; Bohling, J.C.; Arif, A.M.; Gladysz, J.A. *Organometallics* **1999**, *18*, 3261-3263.

58. Dembinski, R.; Bartik, T.; Bartik, B.; Jaeger, M.; Gladysz, J.A. *J. Am. Chem. Soc.* **2000**, *122*, 810-822.

59. Meyer, W.E.; Amoroso, A.J.; Horn, C.R.; Jaeger, M.; Gladysz, J.A. *Organometallics* **2001**, *20*, 1115-1127.

60. Mohr, W.; Stahl, J.; Hampel, F.; Gladysz, J.A. *Inorg. Chem.*, **2001**, *40*, 3263-3264.
61. Zheng, Q.; Gladysz, J.A. *J. Am. Chem. Soc.* **2005**, *127*, 10508-10509.
62. Zheng, Q.; Bohling, J.C.; Peters, T.B.; Frisch, A.C.; Hampel, F.; Gladysz, J.A. *Chem. Eur. J.* **2006**, *12*, 6486-6505.
63. Bruce, M.I.; Kramarczuk, K.A.; Zaitseva, N.N.; Skelton, B.W.; White, A.H. *J. Organomet. Chem.* **2005**, *690*, 1549-1555.
64. Antonova, A.B.; Bruce, M.I.; Ellis, B.G.; Gaudio, M.; Humphrey, P.A.; Jevric, M.; Melino, G.; Nicholson, B.K.; Perkins, G.J.; Skelton, B.W.; Stapleton, B.; White, A.H.; Zaitseva, N.N. *Chem. Commun.* **2004**, 960-961.
65. Ren, T. *Chem. Rev.* **2008**, *108*, 4185-4207.
66. Burgun, A.; Gendron, F.; Roisnel, T.; Sinbandhit, S.; Costuas, K.; Halet, J.-F.; Bruce, M.I.; Lapinte, C. *Organometallics* **2013**, *32*, 1866-1875.
67. Bruce, M.I.; Costuas, K.; Gendron, F.; Halet, J.-F.; Jevric, M.; Skelton, B.W. *Organometallics* **2012**, *31*, 6555-6566.
68. Burgun, A.; Gendron, F.; Schauer, P.A.; Skelton, B.W.; Low, P.J.; Costuas, K.; Halet, J.-F.; Bruce, M.I.; Lapinte, C. *Organometallics* **2013**, *32*, 5015-5025
69. Bruce, M.I.; Burgun, A.; Grelaud, G.; Jevric, M.; Nicholson, B.K.; Skelton, B.W.; White, A.H.; Zaitseva, N.N. *Z. Anorg. Allg. Chem.* **2011**, *637*, 1334-1340.
70. Low, P.J.; Bruce, M.I. *Adv. Organomet. Chem.* **2002**, *48*, 71-288.
71. Nguyen, P.; Zheng, Y.A.; Agocs, L.; Lesley, G.; Marder, T.B. *Inorg. Chim. Acta* **1994**, *220*, 289-296.
72. Batsanov, A.S.; Collings, J.C.; Fairlamb, I.J.S.; Holland, J.P.; Howard, J.A.K.; Lin, Z.Y.; Marder, T.B.; Parsons, A.C.; Ward, R.M.; Zhu, J. *J. Org. Chem.* **2005**, *70*, 703-706.
73. Liu, Q.; Burton, D.J. *Tetrahedron Lett.* **1997**, *38*, 4371-4374.
74. Rossi, R.; Carpita, A.; Bigelli, C. *Tetrahedron Lett.* **1985**, *26*, 523-526.
75. Hay, A.S. *J. Org. Chem.* **1962**, 27, 3320-3321.
76. Bruce, M.I.; Kelly, B.D.; Skelton, B.W.; White, A.H. *J. Organomet. Chem.* **2000**, *604*, 150-156.
77. Bruce, M.I.; Hall, B.C.; Kelly, B.D.; Low, P.J.; Skelton, B.W.; White, A.H. *J. Chem. Soc., Dalton Trans.* **1999**, 3719-3728.

78. Coat, F.; Lapinte, C. *Organometallics* **1996**, *15*, 477-479.
79. Zheng, Q.; Hampel, F.; Gladysz, J.A. *Organometallics* **2004**, *23*, 5896-5899.
80. de Quadras, L; Hampel, F.; Gladysz, J.A. *Dalton Trans.* **2006**, 2929-2933.
81. Peters, T. B.; Zheng, Q.; Stahl, J.; Bohling, J.C.; Arif, A.M.; Hampel, F.; Gladysz, J.A. *J. Organomet. Chem.* **2002,** *641*, 53-61.
82. Bruce, M.I.; Cole, M.L.; Ellis, B.G.; Gaudio, M.; Nicholson, B.K.; Parker, C.R.; Skelton, B.W.; White, A.H. *Polyhedron* **2015**, *86*, 43-56.
83. Bock, S.; Eaves, S.G.; Parthey, M.; Kaupp, M.; Le Guennic, B.; Halet, J.-F.; Yufit, D.S.; Howard, J.A.K.; Low, P.J. *Dalton Trans.*, **2013**, *42*, 4240-4243.
84. Zafert, S.; Gladysz, J.A. *Chem. Rev.* **2006**, *106*, PR1-PR33
85. Schauer, P.A.; Low, P.J. *Eur. J. Inorg. Chem.* **2012**, *3*, 390-411.
86. Bruce, M.I.; Low, P.J.; Costuas, K.; Halet, J.-F.; Best, S.P.; Heath, G.A. *J. Am. Chem. Soc.* **2000**, 122, 1949-1962.
87. Parthey, M.; Gluyas, J.B.G.; Schauer, P.A.; Yufit, D.S.; Howard, J.A.K.; Kaupp, M.; Low, P.J. *Chem. Eur. J.* **2013**, *19*, 9780-9784.
88. Krejcik, M.; Danek, M.; Hartl, F. *J. Electroanal. Chem.* **1991**, *317*, 179-187.
89. Lichtenberger, D.L.; Renshaw, S.K.; Wong, A.; Tagge, C.D. *Organometallics* **1993**, *12*, 3522-3536.
90. Koentjoro, O.F.; Rousseau, R.; Low, P.J. *Organometallics* **2001**, *20*, 4502-4509.
91. Herrmann, C.; Neugebauer, J.; Gladysz, J.A.; Reiher, M. *Inorg. Chem.* **2005**, *44*, 6174-6182.
92. Fox, M.A.; Roberts, R.L.; Khairul, W.M.; Hartl, F.; Low, P.J. *J. Organomet. Chem.* **2007**, *692*, 3277-3290.
93. McGrady, J.E.; Lovell, T.; Stranger, R.; Humphrey, M.G. *Organometallics* **1997**, *16*, 4004-4011.
94. Paul, F.; Ellis, B.G.; Bruce, M.I.; Toupet, L.; Roisnel, T.; Costuas, K.; Halet, J.F.; Lapinte, C. *Organometallics* **2006**, *25*, 649-665.
95. Moreno-García, P.; Gulcur, M.; Manrique, D. Z.; Pope, T.; Hong, W.; Kaliginedi, V.; Huang, C.; Batsanov, A.S.; Bryce, M.R.; Lambert, C.; Wandlowski, T. *J. Am. Chem. Soc.* **2013**, *135*, 12228-12240.
96. Sheldrick, G.M. *Acta Cryst., Sect. A*. **2008**, *64*, 112-122.
97. Dolomanov, O.V.; Bourhis, L.J.; Gildea, R.J.; Howard, J.A.K.; Puschmann, H. *J. Appl. Cryst.* **2009**, *43*, 339-341.

98. Whilst compound **4b** analyzed well, and **6** as a partial CH_2Cl_2 solvate (consistent with the crystallographic work and the ^1H NMR spectrum) the other complexes consistently analyzed very low in carbon. For example **4c**: $C_{52}H_{42}OP_2Ru$ C, 73.83; H, 5.00. Found C, 71.45; H, 4.31. **4d**: $C_{53}H_{42}P_2RuS$ C, 72.84; H, 4.84. Found C, 68.75; H, 4.89. It is known that unsaturated, acetylene-rich compounds can thermally polymerize to give some extraordinarily robust thermoset carbonaceous materials; see, for example, (a) Stephens, E.B.; Tour, J.M. *Adv. Mater.* **1992**, *4*, 570-572 (b) Stephens, E.B.; Tour, J.M. *Macromol.* **1993**, *26*, 2420-2427; (c) Ozaki, J.; Ito, M.; Fukazawa, H.; Yamanobe, T.; Hanaya, M.; Oya, A. *J. Anal. Appl. Pyrol.* **2006**, *77*, 56-62). Although we do not wish to be drawn on undue speculation, the low carbon analysis is at least consistent with formation of such thermoset materials during thermal analysis.

99. Gaussian 09, Revision A.02, Frisch, M. J.; Trucks, G. W.; Schlegel, H. B.; Scuseria, G. E.; Robb, M. A.; Cheeseman, J. R.; Scalmani, G.; Barone, V.; Mennucci, B.; Petersson, G. A.; Nakatsuji, H.; Caricato, M.; Li, X.; Hratchian, H. P.; Izmaylov, A. F.; Bloino, J.; Zheng, G.; Sonnenberg, J. L.; Hada, M.; Ehara, M.; Toyota, K.; Fukuda, R.; Hasegawa, J.; Ishida, M.; Nakajima, T.; Honda, Y.; Kitao, O.; Nakai, H.; Vreven, T.; Montgomery, Jr., J. A.; Peralta, J. E.; Ogliaro, F.; Bearpark, M.; Heyd, J. J.; Brothers, E.; Kudin, K. N.; Staroverov, V. N.; Kobayashi, R.; Normand, J.; Raghavachari, K.; Rendell, A.; Burant, J. C.; Iyengar, S. S.; Tomasi, J.; Cossi, M.; Rega, N.; Millam, J. M.; Klene, M.; Knox, J. E.; Cross, J. B.; Bakken, V.; Adamo, C.; Jaramillo, J.; Gomperts, R.; Stratmann, R. E.; Yazyev, O.; Austin, A. J.; Cammi, R.; Pomelli, C.; Ochterski, J. W.; Martin, R. L.; Morokuma, K.; Zakrzewski, V. G.; Voth, G. A.; Salvador, P.; Dannenberg, J. J.; Dapprich, S.; Daniels, A. D.; Farkas, O.; Foresman, J. B.; Ortiz, J. V.; Cioslowski, J.; Fox, D. J. *Gaussian, Inc.*, Wallingford CT, 2009.

100. (a) Becke, A.D. *J. Chem. Phys.* **1993**, *98*, 5648-5652. (b) Lee, C.; Yang, W.; Parr, R.G. *Phys. Rev. B* **1988**, *37*, 785-789.

101. (a) Petersson, G.A.; Al-Laham, M.A. *J. Chem. Phys.* **1991**, *94*, 6081-6090. (b) Petersson, G.A.; Bennett, A.; Tensfeldt, T.G.; Al-Laham, M.A.; Shirley, W.A.; Mantzaris, J. *J. Chem. Phys.* **1988**, *89*, 2193-2218.

102. (a) V. Barone, M. Cossi, *J. Phys. Chem. A* **1998**, *102*, 1995-2001. (b) M. Cossi, N. Rega, G. Scalmani, V. Barone, *J. Comput. Chem.* **2003**, *24*, 669-681.

103. GaussView 5.0, Dennington, R. D.; Keith, T. A.; Millam, J. M. *Gaussian, Inc*, Wallingford CT, 2008.

104. O'Boyle, N. M., Tenderholt, A. L.; Langner, K. M. *J. Comp. Chem*. **2008**, *29*, 839-845.

105. Ditchfield, R. *Mol. Phys.* **1974**, *27*, 789-807; Rohling,. C. M.; Allen, L. C.; Ditchfield, R. *Chem. Phys.* **1984**, *87*, 9-15; Wolinski, K.; Hinton, J. F.; Pulay, P. *J. Am. Chem. Soc.* **1990**, *112*, 8251-8260.

FOR TABLE OF CONTENTS USE ONLY

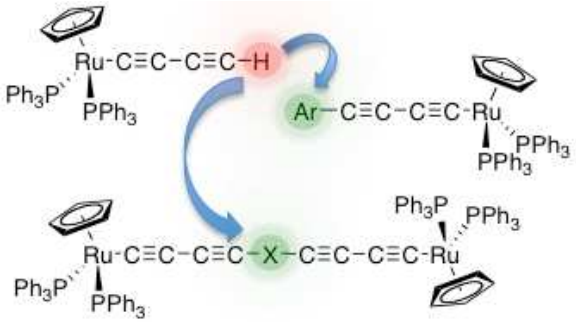

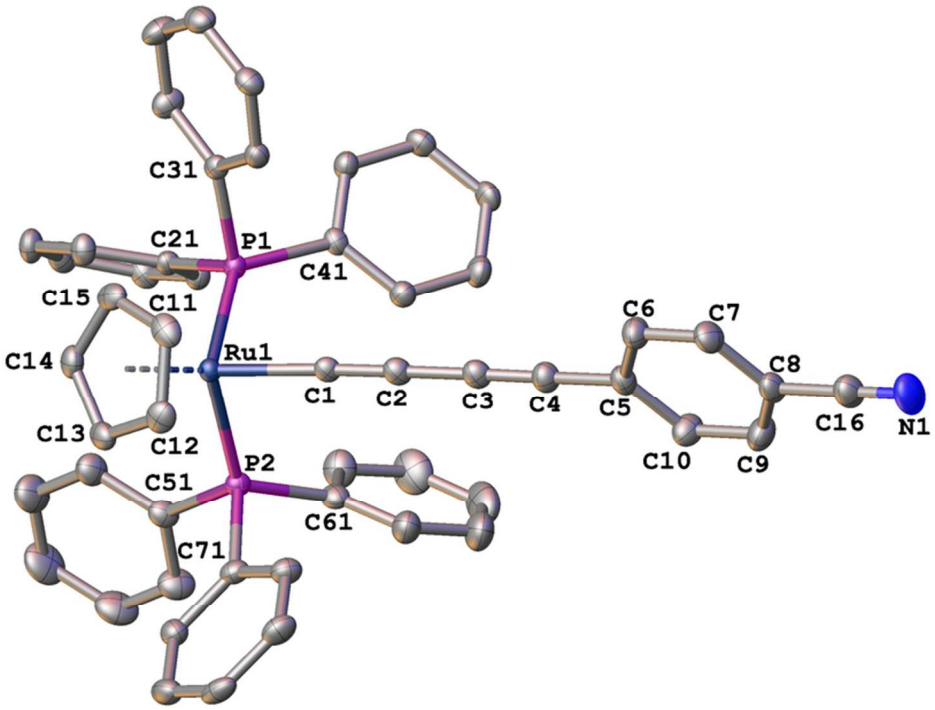

Fig.1 Molecular structure of 4a showing the atom labeling scheme. In this and all subsequent plots thermal ellipsoids are drawn at 50% probability level, H-atoms and solvent molecules are omitted for clarity.
73x53mm (300 x 300 DPI)

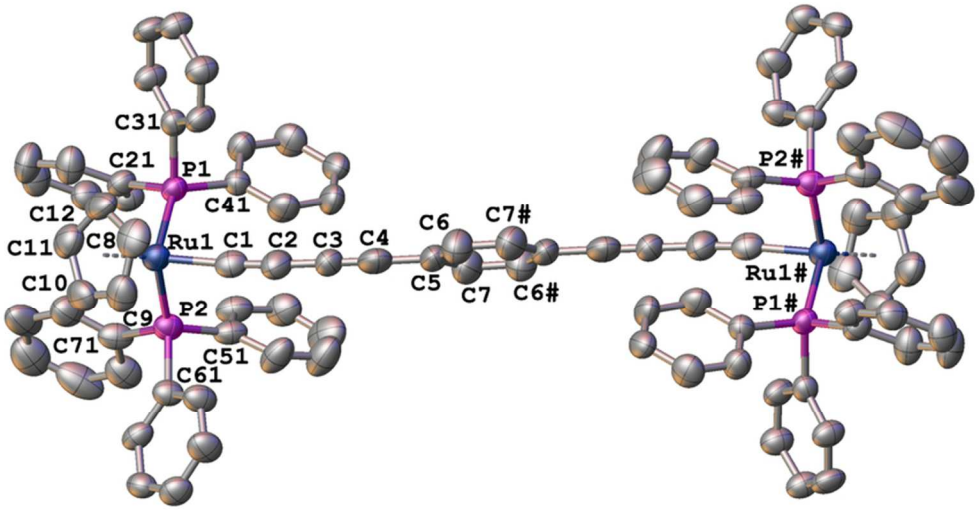

Fig. 2. A plot of a molecule of 5. The molecule is located in the center of symmetry.
73x53mm (300 x 300 DPI)

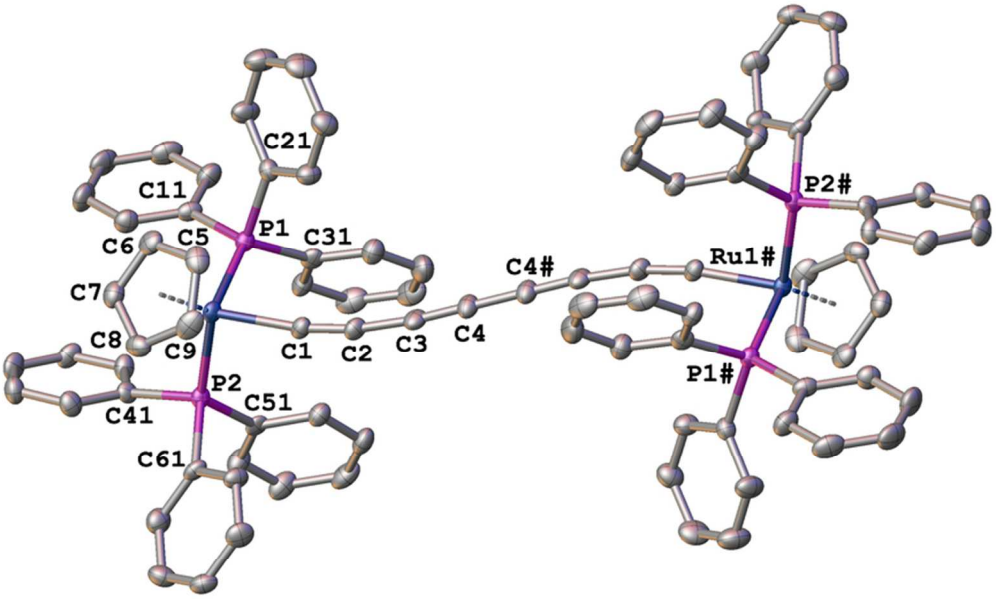

Fig. 3. A plot of a molecule of 6. The molecule is located in the center of symmetry.
73x53mm (300 x 300 DPI)

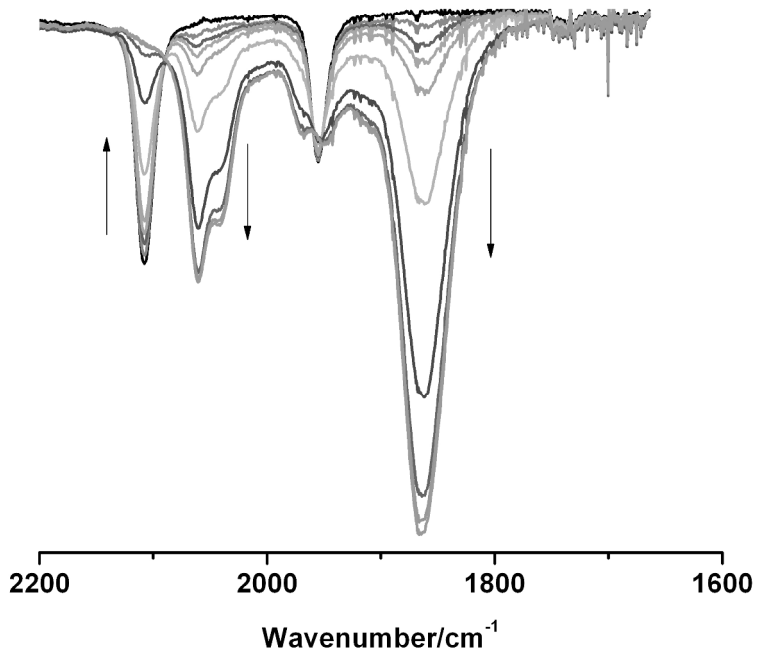

Fig. 4. The IR spectra collected in a spectroelectrochemical cell during oxidation of 6 (0.1 M NBu4PF6 / CH2Cl2).
273x207mm (300 x 300 DPI)

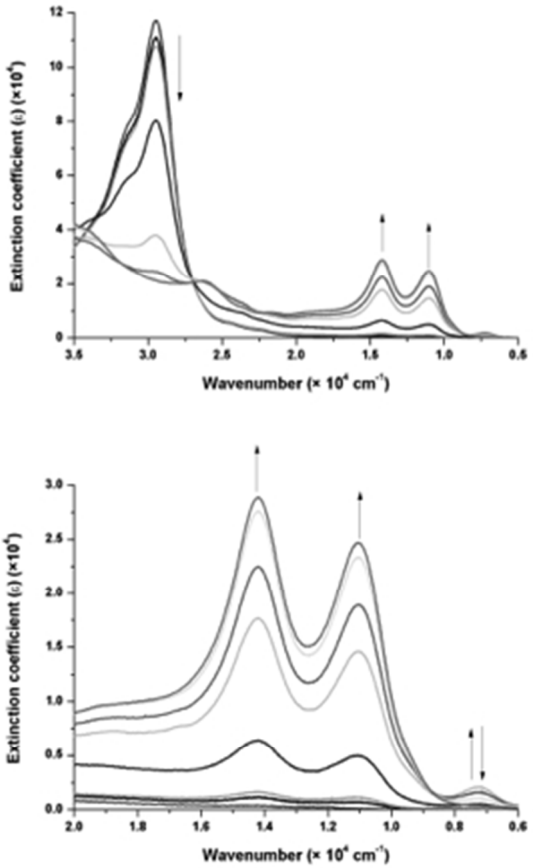

Fig 5. The UV-Vis-NIR spectra collected in a spectroelectrochemical cell during oxidation of 6 (0.1 M NBu4PF6 / CH2Cl2).
114x166mm (72 x 72 DPI)

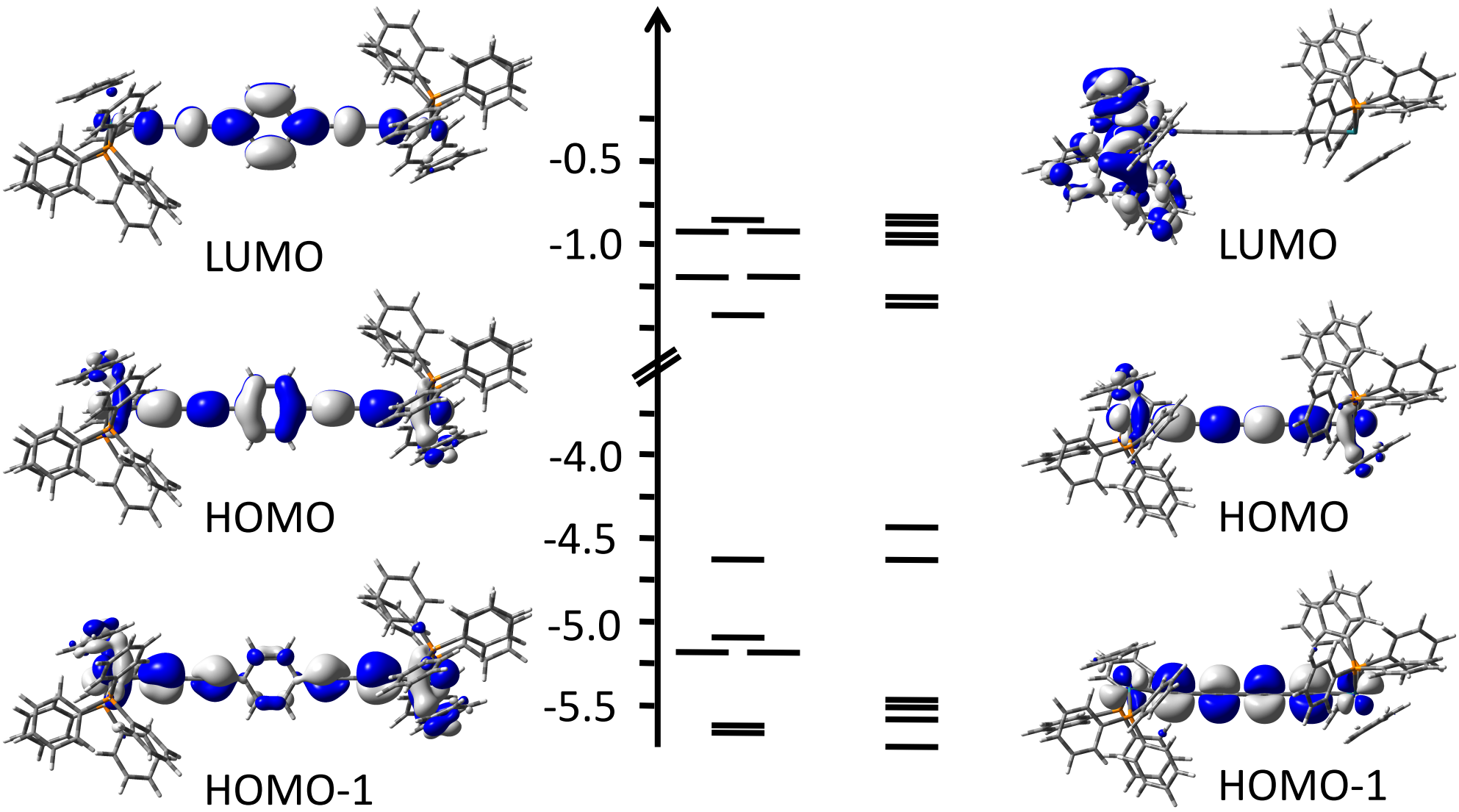
LUMO
HOMO
HOMO-1
-0.5
-1.0
-4.0
-4.5
-5.0
-5.5
LUMO
HOMO
HOMO-1

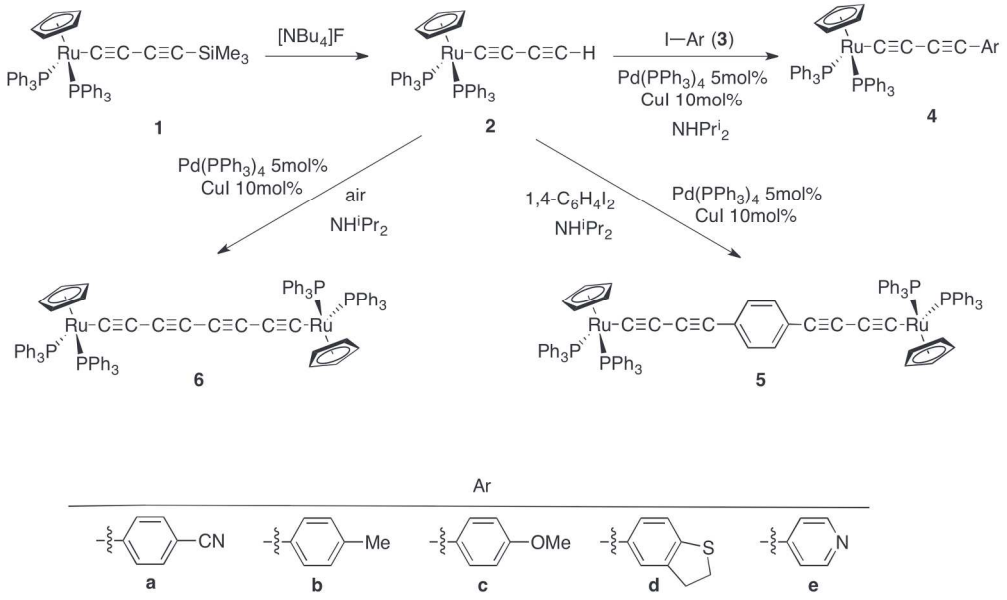

188x112mm (300 x 300 DPI)

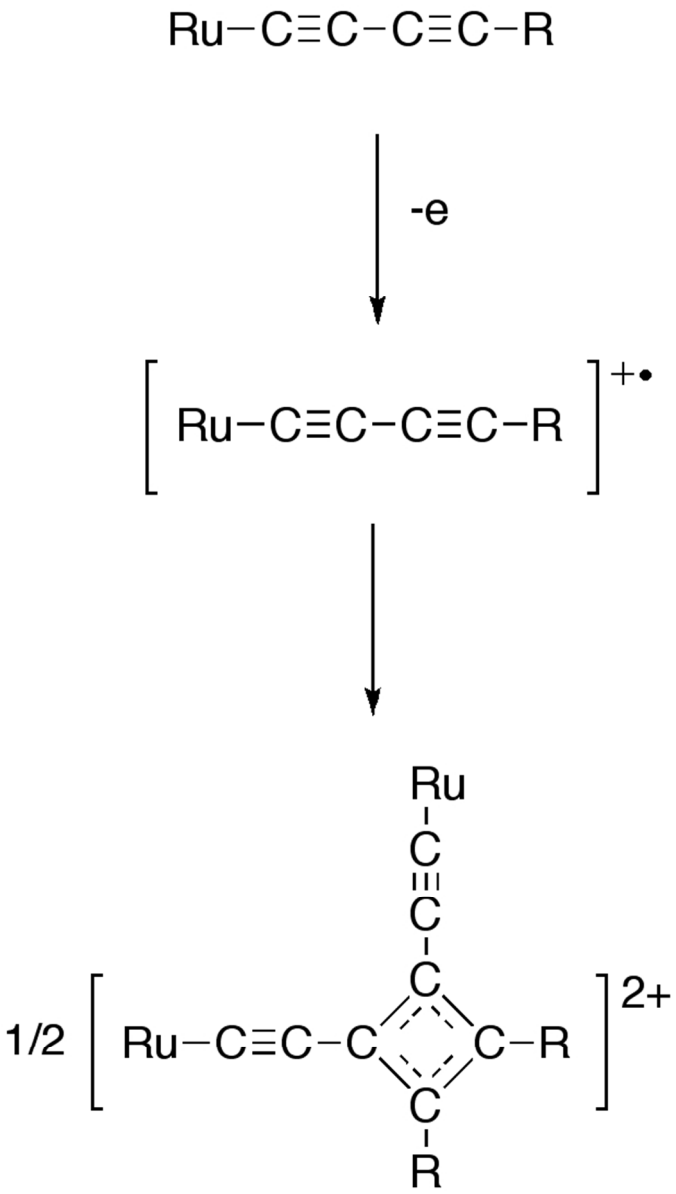

Scheme 2. A general oxidation and dimerization process for a Ru-C≡C-C≡C-R complex [Ru = Ru(PP)Cp´ where PP = (PPh3)2 or dppe, Cp´ = Cp or Cp*; R = aryl or -(C≡C)n-Ru].
53x93mm (300 x 300 DPI)

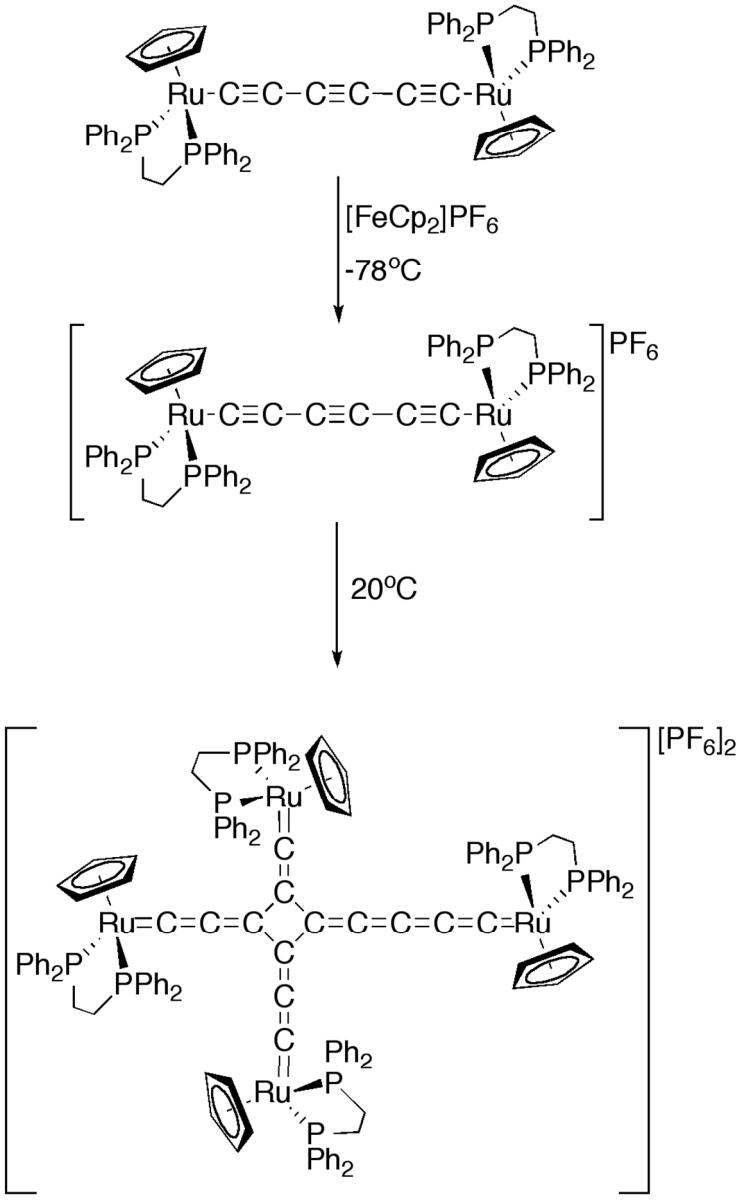

Scheme 3. The synthesis and dimerization of [{Ru(dppe)2Cp}2(μ-C≡CC≡CC≡C)]+.68
87x141mm (300 x 300 DPI)

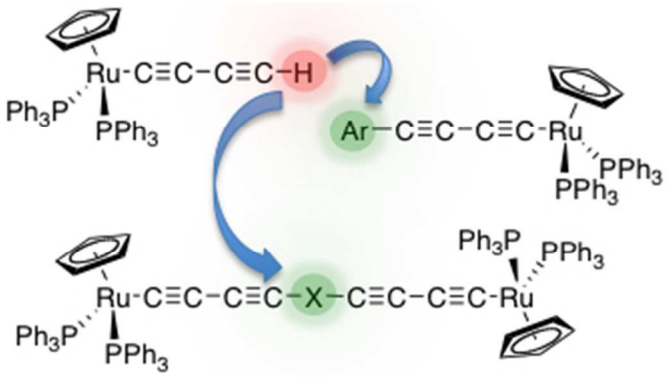

For Table of Contents Use Only
118x65mm (72 x 72 DPI)